Original Article

Clinical impact of targeted amplicon sequencing for meningioma as a practical clinical sequencing system

Authors and affiliations:

Sayaka Yuzawa[1], Hiroshi Nishihara[2, 3], Shigeru Yamaguchi[4], Hiromi Mohri[1], Lei Wang[2], Taichi Kimura[2, 3], Masumi Tsuda[1], Mishie Tanino[1], Hiroyuki Kobayashi[4], Shunsuke Terasaka[4], Kiyohiro Houkin[3, 4], Norihiro Sato[3], Shinya Tanaka[1, 2].

[1]Department of Cancer Pathology, Hokkaido University Graduate School of Medicine, Sapporo, Japan.

[2]Department of Translational Pathology, Hokkaido University Graduate School of Medicine, Sapporo, Japan.

[3]Translational Research Laboratory, Hokkaido University Hospital, Clinical Research and Medical Innovation Center, Sapporo, Japan.

[4]Department of Neurosurgery, Hokkaido University Graduate School of Medicine, Sapporo, Japan.

Corresponding author:

Hiroshi Nishihara, MD., PhD.

Department of Translational Pathology, Hokkaido University Graduate School of Medicine, North 15, West 7, Kita-ku, Sapporo, 060-8638, Japan.

E-mail: hnishihara@med.hokudai.ac.jp

Tel: +81-11-706-5053

Fax: +81-11-706-5902

Running title: Clinical sequencing of meningioma

Abstract

Recent genetic analyses using next-generation sequencers have revealed numerous genetic alterations in various tumors including meningioma, which is the most common primary brain tumor. However, their use as routine laboratory examinations in clinical applications for tumor genotyping is not cost effective. To establish a clinical sequencing system for meningioma and investigate the clinical significance of genotype, we retrospectively performed targeted amplicon sequencing on 103 meningiomas and evaluated the association with clinicopathological features. We designed amplicon sequencing panels targeting eight genes including *NF2*, *TRAF7*, *KLF4*, *AKT1*, and *SMO*. Libraries prepared with genomic DNA extracted from PAXgene-fixed paraffin-embedded tissues of 103 meningioma specimens were sequenced using the Illumina MiSeq. *NF2* loss in some cases was also confirmed by interphase-fluorescent *in situ* hybridization. We identified *NF2* loss and/or at least one mutation in *NF2*, *TRAF7*, *KLF4*, *AKT1*, and *SMO* in 81 out of 103 cases (79%) by targeted amplicon sequencing. Based on genetic status, we categorized meningiomas into three genotype groups: NF2 type, TRAKLS type harboring mutation in *TRAF7*, *AKT1*, *KLF4*, and/or *SMO*, and "not otherwise classified" type. Genotype significantly correlated with tumor volume, tumor location, and MRI findings such as adjacent bone change and heterogeneous gadolinium enhancement, as well as histopathological subtypes. In addition, multivariate analysis revealed that genotype was independently associated with risk of recurrence. In conclusion, we established a rapid clinical sequencing system that enables final confirmation of meningioma genotype within 7 days turnaround time. Our method will bring multiple benefits to neuropathologists and neurosurgeons for accurate diagnosis and appropriate postoperative management.

Introduction

Meningioma, arising from meningothelial cells, is the most common primary brain tumor and accounts for about 25% of all intracranial tumors (1). Although most such tumors are categorized as World Health Organization (WHO) grade I, these histopathologically benign tumors sometimes recur despite complete surgical resection (2). In fact, the 10 year recurrence rate of WHO grade I meningioma after gross total resection reaches 15%–20% (3). Moreover, atypical (grade II) or anaplastic (grade III) meningiomas, which account for about 20% of all meningiomas (2), show a more aggressive clinical course; 50% and 80% of WHO grade II and III meningiomas recur within 5 years, respectively (4). Recurrent meningiomas often become resistant against surgery or radiation therapy. Therefore, appropriate evaluation of the recurrent risk at initial diagnosis is important.

The development of next-generation sequencers has enabled researchers to perform genetic investigations of various tumors, resulting in the discovery of numerous clinically relevant mutations and/or copy number alterations. Loss of *neurofibromin 2* (*NF2*) has been found in about half of sporadic meningiomas (5-7), and mutations in *TRAF7*, *KLF4*, *AKT1,* and *SMO* were recently reported in non-NF2 meningiomas by next-generation sequencing (8). Loss of *NF2* has been evaluated mainly by karyotyping (9), comparative genomic hybridization (10), fluorescent *in situ* hybridization (11), single nucleotide polymorphism array (11), and quantitative polymerase chain reaction analysis (12); and additional genetic analyses are required to investigate mutations in other genes. The combination of these methods leads to increased cost and number of days required for analysis, so the application of these techniques for regular laboratory examinations remains to be established.

In this study, we performed targeted amplicon sequencing of 103 meningioma specimens and evaluated the association with genotype and clinicopathological features using the desktop sequencer MiSeq, and established a clinical sequencing system for meningioma to determine the genotype as a routine laboratory examination in addition to concurrent pathological diagnosis.

Materials and methods

Patients

Frozen tumor samples of 103 patients surgically resected in 1988–2015 were used for genetic analyses. Clinicopathological features are summarized in Table 1 and Supplementary Table 1. The patients included 31 men and 72 women with a median age of 55 years (range 15–87) at surgery. Eighty-two samples were newly diagnosed meningiomas and 21 were recurrent meningiomas, eight of which were specimens obtained after radiation therapy. Hematoxylin and eosin (H&E) staining and immunohistochemistry with a monoclonal anti-Ki-67 antibody (1:100 dilution, clone MIB-1, M7240, DAKO, Glostrup, Denmark) were performed with PAXgene-fixed paraffin-embedded tissue obtained from the snap-frozen specimens in all cases and corresponding formalin-fixed paraffin-embedded tissue in some cases. Histological diagnosis was reviewed according to the current WHO classification 2007 (13) by two experienced pathologists (S. Yuzawa and H. Nishihara) . Among the 82 patients with newly diagnosed meningioma, preoperative magnetic resonance imaging (MRI) information was obtained from 72 patients. Clinical follow-up data were obtained from 90 patients. Recurrence-free survival in the recurrent specimens was measured by the time from the first operation to the recurrence. Sampling, storage, and analysis of the tumor samples included

in this study were approved by the Internal Review Board on Ethical Issues of Hokkaido University Hospital and Graduate School of Medicine, Sapporo, Japan. Written informed consent was obtained from all patients in this study.

DNA extraction and quantification

Frozen tumor samples (median size in diameter 7 mm, range 2.5–12) were fixed with PAXgene Tissue System (PreAnalytiX, Hombrechtikon, Switzerland) and embedded in paraffin according to the manufacturer's protocol. Genomic DNA was extracted from PAXgene-fixed paraffin-embedded tissues using the PAXgene Tissue DNA Kit (PreAnalytiX), following the manufacturer's instructions. For the control of copy number alterations, genomic DNA was extracted from the blood of three healthy volunteers using the QIAamp DNA Mini Kit (Qiagen, Hilden, Germany). The quality of genomic DNA was assessed using the Qubit dsDNA BR assay kit and the Qubit fluorometer 2.0 (Invitrogen, Carlsbad, CA, USA), and the GeneRead DNA QuantiMIZE Assay Kit (Qiagen).

Targeted amplicon sequencing and data analysis

An amplicon sequencing panel targeting the entire exonic sequence of six genes (*NF2*, *AKT1*, *SMO*, *ERBB2*, *KIT*, and *MET*) was designed by a GeneRead Mix-n-Match panel (181905 MNGHS-00062X-296; Qiagen) and a custom panel targeting the whole exon of *TRAF7* and partial exon of *KLF4* (targeting *KLF4* K409Q) was generated by a GeneRead Custom panel (181902 CNGHS-00120X-44; Qiagen). The GeneRead DNAseq Targeted Panel V2 (Qiagen) was used for library preparation with 59–473 ng of genomic DNA following the manufacturer's instructions. The quality of libraries was assessed using an Agilent 2100 bioanalyzer and Agilent DNA 1000 Kit (Agilent, Santa Clara, CA, USA), and the GeneRead Library Quant Kit (Qiagen). The libraries were sequenced using the Illumina MiSeq to produce 150-bp paired-end reads.

The raw read data obtained from amplicon sequencing were processed by online analytical resources from the GeneRead DNAseq Variant Calling Service (http://ngsdataanalysis.sabiosciences.com/NGS2/) for analysis of mutations and copy number alterations. In addition, BAM files obtained from the GeneRead DNAseq Variant Calling Service were processed by BioReT System (Amelieff, Tokyo, Japan) for analysis of mutations. In BioReT System, BAM files were realigned and recalibrated with the GATK (Genome Analysis Toolkit) (version 1.6.13), using RealignerTargetCreator, IndelRealigner, CountCovariates, and TableRecalibration. Single nucleotide variants and small indels were detected using the GATK UnifiedGenotyper, followed by filtering for low-quality variants using the GATK VariantFiltration. All analyses were performed with default settings except for the minIndelFrac parameter for indel call using GATK UnifiedGenotyper, which was set to 0.05. After variant detection, VCF files were annotated by SnpEff genetic variant annotation and effect prediction toolbox (version 4.0). Information about Catalogue of Somatic Mutations in Cancer (COSMIC) database (version 72) and IntOGen (version 1412) was annotated using SnpSift, a package tool of SnpEff, to VCF and variants on targeted genes were extracted. Single nucleotide variants were limited to protein-altering mutations at ≥10% variant frequency with read depth of >100. Germline variants, except in the *NF2* gene, were manually excluded according to variant frequency and by referencing to dbSNP and Human Genetic Variation Database (HGVD).

Fluorescent *in situ* hybridization analysis

The formalin-fixed paraffin-embedded tissues of 35 tumors were examined by interphase-fluorescent *in situ* hybridization (I-FISH) with commercially available probes for 22q (FG0003, Abnova, Taipei, Taiwan). For microscopic evaluation, 200 interphase nuclei were examined for each specimen.

Statistical analysis

Kruskal–Wallis one-way analysis of variance test with the Steel–Dwass test for post hoc determination and χ^2 analysis were performed to analyze the correlations between mutation subtype and clinical data. For survival analysis, Kaplan–Meier analysis and the log-rank test were used. Cox proportional hazards model was used for univariate and multivariate survival analysis to adjust for covariates of statistical significance, including age, sex, Simpson grade, WHO grade, and genotype. Analyses were performed on Ekuseru-Toukei 2015 (Social Survey Research Information Co., Tokyo, Japan) and JMP version 11.2 (SAS Institute, Cary, NC, USA). $P < 0.05$ was considered statistically significant.

Results

Copy number alteration analyses by next-generation sequencing and fluorescent *in situ* hybridization

The results of interphase-fluorescent *in situ* hybridization were available in 34 out of 35 samples investigated. Nineteen cases (56%) displayed a diploid karyotype. Thirteen cases (38%) showed monosomy 22 in 60%–100% of the interphase nuclei, whereas del(22q) was observed in 12%–20% of the interphase nuclei in the other two cases (6%) (Supplementary Figure 1 and Supplementary Table 2).

In copy number variant calling workflow of next-generation sequencing, 71 of 103 cases (69%) showed a score *Q* of *NF2* above 50, indicating strong evidence for *NF2* loss (14). One case displayed a pattern of biallelic loss (Supplementary Figure 1J); interphase-fluorescent *in situ* hybridization was not applicable to this case because of the age of the formalin-fixed paraffin-embedded tissue (obtained in 1996).

The receiver operating characteristic curve for next-generation sequencing against interphase-fluorescent *in situ* hybridization is shown in Supplementary Figure 2. The area under the curve was 0.783. The score $Q = 79$ presented maximum Youden index with sensitivity as 86.7% and specificity as 73.7%. The positive rates in the 34 cases whose results of interphase-fluorescent *in situ* hybridization were available were 52.9% using next-generation sequencing and 44.1% interphase-fluorescent *in situ* hybridization. Cases with discordant results between next-generation sequencing and interphase-fluorescent *in situ* hybridization (next-generation sequencing positive, interphase-fluorescent *in situ* hybridization negative in five cases; next-generation sequencing negative, interphase-fluorescent *in situ* hybridization positive in two cases) displayed no difference in score *Q* or score *P* compared with cases with concordant results (Supplementary Figure 1K–R). Overall, 62 of 103 cases (60%) showed *NF2* loss when using the cutoff value (score $Q \geq 79$). Twenty-six copy number alterations of *AKT1*, *SMO*, *MET*, *KIT,* and *ERBB2* genes were observed in 22 cases (21%) based on next-generation sequencing, but the accuracy of copy number alterations in these genes was not confirmed by interphase-fluorescent *in situ* hybridization. Loss of *AKT1*, *KIT*, *SMO,* and *MET* were detected in four, four, five, and five of 103 cases, respectively, whereas amplification of *KIT*, *MET,* and *ERBB2* were observed in three, four, and one cases, respectively (Figure 1 and Supplementary Table 2).

Mutation analysis

In total, 71 protein-altering mutations were detected in 57 out of 103 cases (55%) (Figure 1 and Supplementary Table 3). Thirty-nine cases (38%) harbored *NF2* mutations, and one of these cases carried two different frameshift mutations. Mutation types of *NF2* were variable: frameshift mutation in 19 cases, splice region mutation in 10 cases, nonsense mutation in nine cases, and in-frame deletion in one case. Thirty-eight of 62 cases (61%) with *NF2* loss simultaneously carried *NF2* mutation

(Figure 2A). Two tumors from the patients with Neurofibromatosis type 2 carried both *NF2* loss and *NF2* mutation. Two of three patients with radiotherapy-induced meningioma carried *NF2* loss, one of which harbored concomitant mutation in *NF2*, whereas the other patient did not show any mutations or *NF2* loss. Missense mutations in *TRAF7*, *KLF4*, *AKT1,* and *SMO* were observed in 16 (16%), eight (8%), five (5%), and one (1%) cases, respectively (Figures 1 and 2A). All *AKT1* and *KLF4* mutations corresponded to E17K and K409Q mutations, respectively. *KLF4* K409Q always co-occurred with mutations of *TRAF7. AKT1* E17K was accompanied by *TRAF7* mutation in all but one case, which was the case of chordoid meningioma (Supplementary Figure 3E). With regard to mutation in *TRAF7*, the reproducible mutations, *TRAF7* N520S and R641H, were detected in five and two cases, respectively, while the other nine mutations differed from each other. Nine of 11 mutations in *TRAF7* mapped to the WD40 domains. Mutations in *TRAF7*, *KLF4*, *AKT1,* and *SMO* were mutually exclusive of *NF2* mutation and *NF2* loss. Consequently, 81 out of 103 cases (79%) carried at least one or more gene alterations including mutations in the five genes and/or *NF2* loss. No somatic mutation was detected in *KIT*, *MET,* or *ERBB2*. These analyses of mutation and copy number alterations could be completed within 7 days from tumor tissue fixation.

Clinicopathological analysis based on genotype

To investigate the relationship between clinicopathological features and genotype, we classified meningioma into three categories based on genotype obtained by next-generation sequencing: NF2 type, TRAKLS type, and “not otherwise classified” (NOC) type. NF2 type included cases with *NF2* loss and/or *NF2* mutation. TRAKLS type includes cases with mutation in *TRAF7*, *AKT1*, *KLF4,* and/or *SMO*, and NOC type included cases without any mutation or *NF2* loss in our panel. We classified two cases with loss of *AKT1* or *SMO* but no other mutations into NOC type rather than TRAKLS type, because the loss of these

genes usually causes loss of function, whereas mutations of *AKT1* (E17K) or *SMO* (W535L and L412F) found in TRAKLS type have been considered to activate each downstream signaling.

Statistical analysis revealed that genotype was associated with tumor location ($P = 0.013$, χ^2 analysis,). About 80% of tumors in calvarium were classified as NF2 type (Figure 2B and Supplementary Figure 3A–B), while tumors of TRAKLS type were frequently localized in the skull base (15/18 cases, 83%) (Table 1, Figure 2B, and Supplementary Figure 3C–F). In addition, the size of the tumors in NF2 type was significantly larger than that of those in TRAKLS type (median tumor size 50.3 ml vs. 14.2 ml, respectively; $P < 0.001$, Kruskal–Wallis test) (Figure 2C). The difference in tumor size of NF2 type and TRAKLS type was also statistically significant when limited in the skull base meningiomas (median tumor size 53.9 ml vs. 13.0 ml, respectively; $P < 0.001$). Genotype showed relationships with some imaging characteristics. Calcification ($P = 0.006$, χ^2 analysis), adjacent bone change ($P = 0.001$) and heterogeneous gadolinium enhancement ($P = 0.001$) were more frequently observed in tumors of NF2 type (Table 2). Age and sex were not associated with genotype (Table 1).

Genotype also correlated with histological features. All 23 fibrous meningioma cases, including one case with brain invasion, were classified as NF2 type. All seven cases with secretory components were categorized as TRAKLS type, especially with duplicated mutations in both *TRAF7* and *KLF4*. In contrast, a microcystic component was not observed in TRAKLS type. Ki-67 labeling index (LI) of NF2 type was significantly higher compared with TRAKLS type ($P = 0.002$, Kruskal–Wallis test). Meningiomas of WHO grade II and III were more likely to be NF2 type (56% in WHO grade I vs. 78% in WHO grade II and III), but this was not statistically significant.

Prognostic analyses

Among the 90 patients with clinical follow-up data available, the median follow-up time was 25.1 months (range 1–310) with a median recurrent time of 38.3 months (range 2.5–272). Thirty out of 90 cases (33%) underwent tumor recurrence [25/52 (48%) of NF2 type, 0/18 (0%) of TRAKLS type, and 5/20 (25%) of NOC type] and nine of 88 cases (10%) were deceased [8/50 (16%) of NF2 type, 0/18 (0%) of TRAKLS type, and 1/20 (5%) of NOC type].

Based on Kaplan–Meier analysis, recurrence-free survival for patients of TRAKLS type was significantly better compared with NF2 and NOC type ($P = 0.037$, log-rank test) (Figure 2D). The median recurrence-free survival of NF2 type and NOC type was 3.39 and 12.41 years, respectively. The median recurrence-free survival had not been reached at the time of analysis in patients with TRAKLS type because no one underwent tumor recurrence. The patients with lower Simpson grade (Simpson grade 1–2) and those with WHO grade I showed longer recurrence-free survival than those with higher Simpson grade (Simpson grade 3–4) ($P < 0.001$) and WHO grade II–III ($P < 0.001$), respectively (Supplementary Figure 4). Meningiomas with higher proliferative index (Ki-67 LI ≥ 4) tended to show shorter recurrence-free survival compared with those with lower proliferative index (Ki-67 LI < 4), although log-rank test did not reveal a statistical significance ($P = 0.079$) (Supplementary Figure 4).

The multivariate analysis using the Cox proportional hazard models revealed that genotype was independently associated with recurrent risk after adjustment for Simpson Grade, Ki-67 LI, and WHO grade (NF2 type vs. TRAKLS type, HR = 2.60×10^9, 95% CI = 2.05 to infinity, $P = 0.008$) (Supplementary Table 4).

Discussion

The application of next-generation sequencing as a routine laboratory examination is challenging owing to cost-effectiveness. Numerous studies using next-generation sequencers have revealed clinically relevant genetic alterations in various tumors, and some researchers have recently advocated the clinical use of next-generation sequencers (15-20). This is the first study to establish a clinical sequencing system for meningioma, which is the most common brain tumor.

We investigated the genotype of 103 meningiomas by targeted amplicon sequencing, in which 79% (81/103) of cases carried at least one or more mutations in *NF2*, *TRAF7*, *AKT1*, *KLF4,* and *SMO*, and/or loss of *NF2*. These findings are compatible with a previous report in terms of proportion (79%, 237/300) and the unique pattern of gene alterations (8), thus helping to confirm the technical accuracy of our sequencing method. In terms of histological findings, we also confirmed the genotype-oriented histological pattern: all fibrous meningiomas were classified into NF2 type, and secretory component was associated with mutation in *TRAF7* and *KLF4*; these trends were similar to previous reports (9, 21, 22). In addition, tumor size of NF2 type was larger than that of TRAKLS types, probably because of high proliferative ability. In fact, NF2 type meningioma showed higher Ki-67 LI compared with TRAKLS type, and this result is compatible with previous studies showing the relationship between NF2 and Ki-67 LI (23, 24). Meningiomas of NF2 type also showed characteristic findings in MRI such as calcification, adjacent bone change, and heterogeneous gadolinium enhancement, indicating that preoperative MRI findings including location and size, could be potential predictors for tumor genotype.

The recent establishment of an algorithm to analyze copy number alterations by amplicon sequencing (14) has expanded the application of targeted amplicon sequencing. Current, reliable, clinically practical methods to investigate copy number alterations include interphase-fluorescent *in situ* hybridization and quantitative polymerase chain reaction analysis; however,

mutations cannot be simultaneously confirmed with these methods. The amplicon sequencing system we employed in this study yielded valuable results of copy number alterations in addition to mutations. Loss of *NF2*, which was found in 40%–60% of sporadic meningioma (5-7, 10), was observed in 60% of our cases. Interphase-fluorescent *in situ* hybridization for *NF2* was also performed in 35 out of 103 cases (34%) and the concordance rate between the results of interphase-fluorescent *in situ* hybridization and next-generation sequencing was 79%. Four out of five cases with *NF2* diploid by interphase-fluorescent *in situ* hybridization but loss by next-generation sequencing carried protein-altering mutations in *NF2*. Almost all cases with mutations in *NF2* have been shown to carry *NF2* loss simultaneously (10, 11, 25-28). Therefore, the result of interphase-fluorescent *in situ* hybridization in these cases could be a false negative, suggesting the higher sensitivity and specificity of the amplicon sequencing system for copy number alterations. By contrast, one case showed monosomy 22 by interphase-fluorescent *in situ* hybridization but did not show *NF2* loss by next-generation sequencing, indicating the value of interphase-fluorescent *in situ* hybridization as a laboratory examination for copy number alterations.

NF2 inactivation is suggested to be an early event in sporadic meningioma pathogenesis (2, 29), but these gene alterations have been described to poorly correlate with prognosis. In fact, no significant difference in recurrence time was observed between patients with and without loss of 22q (30, 31). Conversely, the association between prognosis and mutations of *TRAF7*, *AKT1*, *KLF4,* and *SMO*, called the TRAKLS type in this study, have never been investigated. Here we revealed that genotype was associated with recurrence independently from the degree of surgical resection completeness (Simpson grade) and histological malignancy (Ki-67 LI and WHO grade), which is known as prognostic factors in meningioma (32-34). TRAKLS type was the most favorable genotype, so in addition to evaluating *NF2* status, identifying this genotype from non-

NF2 meningioma may help the accurate assessment of the recurrent risk. More recently, *TERT* promoter and PIK3CA mutations were reported to be associated with highly aggressive behavior or tumorigenesis in meningioma (35-37). The additional alteration of these genes might be responsible for the recurrence of meningioma or even for the tumorigenesis of NOC type, although additional investigations for these gene mutations in association with the genetic status of *NF2*, *TRAF7*, *AKT1*, *KLF4*, and *SMO* are needed. Genotypes obtained from the clinical sequencing system would be useful for postoperative management, such as determination of follow-up interval or early postoperative radiotherapy, which was previously reported to improve the prognosis of patients with meningioma (38, 39). The shorter turnaround time of our clinical sequencing system, within 7 days after surgery, will provide clinical benefit to patients in terms of seamless genotype-oriented treatment after surgery (Figure 3).

Clinically relevant actionable mutations have been found in various tumors, such as *EGFR* L858R in lung cancer (40), *KRAS* G12D in colorectal cancer (41), and *BRAF* V600E in melanoma (42). Patients with tumors carrying these actionable mutations have been treated effectively with appropriate medicines including molecular targeted therapy. In meningiomas, mutations in *SMO* and *AKT1* may be predictive biomarkers of some molecular targeted drugs such as Hedgehog inhibitors and AKT inhibitors (43). Although patients with these gene mutations showed better prognosis, these tumors are frequently located in the skull base. When the tumor is difficult to completely resect because of its location, Hedgehog inhibitors or AKT inhibitors could be considered as a treatment agent. Therefore, establishing a clinical sequencing system is also crucial for providing personalized medicine.

Quality control of DNA is a crucial problem for the clinical sequencing system. We used PAXgene-fixed paraffin-embedded tissues owing to the high quality of DNA extracted from PAXgene-fixed paraffin-embedded specimens (44, 45) and conserved histological morphology (46). In fact, we analyzed two cases of meningioma using genomic DNA extracted from formalin-fixed paraffin-embedded tissue and obtained similar but imprecise results of copy number alterations (data not shown), mostly because of DNA fragmentation by formalin fixation (47-49). For an appropriate clinical sequencing system, concomitance of conserved histology and high quality nucleotide extraction must be achieved, therefore an alternative sample preparation method, other than snap-frozen or formalin fixation, such as the PAXgene Tissue System, would be considered. Application of our system to widely used formalin-fixed paraffin-embedded tissue would require fine-tuning of some thresholds such as variant frequency for mutation analysis or score Q for copy number alteration analysis.

In conclusion, we established a rapid clinical sequencing system for meningioma by targeted amplicon sequencing. The genotypes obtained by this system were significantly associated with clinicopathological features including histological subtypes, tumor size, MRI findings, and recurrence-free survival. The prevalence of such a clinical sequencing system will bring multiple benefits to meningioma patients by means of more accurate diagnosis and individualized medicine.

Disclosure/Conflict of Interest

The authors declare no conflict of interest.

Acknowledgments

We thank Mr. Jun Moriya (Hokkaido University Graduate School of Medicine) for his technical assistance.

Supplementary information

Supplementary Table 1. Clinicopathological and imaging features of all cases.xlsx

Supplementary Table 2. Results of copy number alterations of NF2 by next-generation sequencing and interphase-fluorescent *in situ* hybridization, and copy number alterations of other genes by next-generation sequencing.xlsx

Supplementary Table 3. Detailed results of mutation analysis.xlsx

Supplementary Table 4. Clinicopathological and genetic findings and their association with recurrence.xlsx

Supplementary Figure 1. Results of interphase-fluorescent *in situ* hybridization and copy number alterations by next-generation sequencing of *NF2* in the representative cases.pdf

Supplementary Figure 2. The receiver operating characteristic curve for next-generation sequencing against interphase-fluorescent *in situ* hybridization.pdf

Supplementary Figure 3. Magnetic resonance imaging and hematoxylin and eosin staining of representative cases.pdf

Supplementary Figure 4. Recurrence-free survival according to genotype, Simpson grade, WHO grade, and Ki-67 LI.pdf

Supplementary information is available at *Modern Pathology*'s website.

References

1. Claus EB, Bondy ML, Schildkraut JM*, et al.* Epidemiology of intracranial meningioma. Neurosurgery 2005;57:1088-95.

2. Mawrin C, Perry A. Pathological classification and molecular genetics of meningiomas. J Neurooncol 2010;99:379-91.

3. Ruiz J, Martinez A, Hernandez S*, et al.* Clinicopathological variables, immunophenotype, chromosome 1p36 loss and tumour recurrence of 247 meningiomas grade I and II. Histol Histopathol 2010;25:341-9.

4. Adeberg S, Hartmann C, Welzel T*, et al.* Long-term outcome after radiotherapy in patients with atypical and malignant meningiomas--clinical results in 85 patients treated in a single institution leading to optimized guidelines for early radiation therapy. Int J Radiat Oncol Biol Phys 2012;83:859-64.

5. Ruttledge MH, Sarrazin J, Rangaratnam S*, et al.* Evidence for the complete inactivation of the NF2 gene in the majority of sporadic meningiomas. Nat Genet 1994;6:180-4.

6. Seizinger BR, de la Monte S, Atkins L, Gusella JF, Martuza RL. Molecular genetic approach to human meningioma: loss of genes on chromosome 22. Proc Natl Acad Sci U S A 1987;84:5419-23.

7. Zankl H, Zang KD. Cytological and cytogenetical studies on brain tumors. 4. Identification of the missing G chromosome in human meningiomas as no. 22 by fluorescence technique. Humangenetik 1972;14:167-9.

8. Clark VE, Erson-Omay EZ, Serin A*, et al.* Genomic analysis of non-NF2 meningiomas reveals mutations in TRAF7, KLF4, AKT1, and SMO. Science 2013;339:1077-80.

9. Kros J, de Greve K, van Tilborg A*, et al.* NF2 status of meningiomas is associated with tumour localization and histology. J Pathol 2001;194:367-72.

10. Hansson CM, Buckley PG, Grigelioniene G*, et al.* Comprehensive genetic and epigenetic analysis of sporadic meningioma for macro-mutations on 22q and micro-mutations within the NF2 locus. BMC Genomics 2007;8:16.

11. Tabernero M, Jara-Acevedo M, Nieto AB*, et al.* Association between mutation of the NF2 gene and monosomy 22 in menopausal women with sporadic meningiomas. BMC Med Genet 2013;14:114.

12. Buccoliero AM, Castiglione F, D RDI*, et al.* NF2 gene expression in sporadic meningiomas: relation to grades or histotypes real time-pCR study. Neuropathology 2007;27:36-42.

13. Perry A, Louis DN, Scheithauer BW, Budka H, von Deimling A. Meningiomas, In: Louis DN, Ohgaki H, Wiestler

OD, Cavenee WK, (eds). WHO Classification of Tumours of the Central Nervous System. 4th ed. IARC: Lyon, France; 2007. pp 164-72.

14. Reinecke F, Satya RV, DiCarlo J. Quantitative analysis of differences in copy numbers using read depth obtained from PCR-enriched samples and controls. BMC Bioinformatics 2015;16:17.

15. Al-Rohil RN, Tarasen AJ, Carlson JA*, et al.* Evaluation of 122 advanced-stage cutaneous squamous cell carcinomas by comprehensive genomic profiling opens the door for new routes to targeted therapies. Cancer 2016;122:249-57.

16. Coco S, Truini A, Vanni I*, et al.* Next generation sequencing in non-small cell lung cancer: new avenues toward the personalized medicine. Curr Drug Targets 2015;16:47-59.

17. Johnson DB, Dahlman KH, Knol J*, et al.* Enabling a genetically informed approach to cancer medicine: a retrospective evaluation of the impact of comprehensive tumor profiling using a targeted next-generation sequencing panel. Oncologist 2014;19:616-22.

18. Marrone M, Filipski KK, Gillanders EM, Schully SD, Freedman AN. Multi-marker Solid Tumor Panels Using Next-generation Sequencing to Direct Molecularly Targeted Therapies. PLoS currents 2014;6.

19. Roy-Chowdhuri S, de Melo Gagliato D, Routbort MJ*, et al.* Multigene Clinical Mutational Profiling of Breast Carcinoma Using Next-Generation Sequencing. Am J Clin Pathol 2015;144:713-21.

20. Sahm F, Schrimpf D, Jones DT*, et al.* Next-generation sequencing in routine brain tumor diagnostics enables an integrated diagnosis and identifies actionable targets. Acta Neuropathol 2015. [Epub ahead of print]

21. Reuss DE, Piro RM, Jones DT*, et al.* Secretory meningiomas are defined by combined KLF4 K409Q and TRAF7 mutations. Acta Neuropathol 2013;125:351-8.

22. Wellenreuther R, Kraus JA, Lenartz D*, et al.* Analysis of the neurofibromatosis 2 gene reveals molecular variants of meningioma. Am J Pathol 1995;146:827-32.

23. Antinheimo J, Haapasalo H, Haltia M*, et al.* Proliferation potential and histological features in neurofibromatosis 2-associated and sporadic meningiomas. J Neurosurg 1997;87:610-4.

24. Pavelin S, Becic K, Forempoher G*, et al.* The significance of immunohistochemical expression of merlin, Ki-67, and p53 in meningiomas. Appl Immunohistochem Mol Morphol 2014;22:46-9.

25. De Vitis LR, Tedde A, Vitelli F*, et al.* Screening for mutations in the neurofibromatosis type 2 (NF2) gene in sporadic meningiomas. Hum Genet 1996;97:632-7.

26. Leone PE, Bello MJ, de Campos JM*, et al.* NF2 gene mutations and allelic status of 1p, 14q and 22q in sporadic meningiomas. Oncogene 1999;18:2231-9.

27. Ng HK, Lau KM, Tse JY*, et al.* Combined molecular genetic studies of chromosome 22q and the neurofibromatosis type 2 gene in central nervous system tumors. Neurosurgery 1995;37:764-73.

28. Ueki K, Wen-Bin C, Narita Y, Asai A, Kirino T. Tight association of loss of merlin expression with loss of heterozygosity at chromosome 22q in sporadic meningiomas. Cancer Res 1999;59:5995-8.

29. Riemenschneider MJ, Perry A, Reifenberger G. Histological classification and molecular genetics of meningiomas. Lancet Neurol 2006;5:1045-54.

30. Linsler S, Kraemer D, Driess C*, et al.* Molecular biological determinations of meningioma progression and recurrence. PLoS One 2014;9:e94987.

31. Sulman EP, Dumanski JP, White PS*, et al.* Identification of a consistent region of allelic loss on 1p32 in meningiomas: correlation with increased morbidity. Cancer Res 1998;58:3226-30.

32. Oya S, Kawai K, Nakatomi H, Saito N. Significance of Simpson grading system in modern meningioma surgery: integration of the grade with MIB-1 labeling index as a key to predict the recurrence of WHO Grade I meningiomas. J Neurosurg 2012;117:121-8.

33. Yamaguchi S, Terasaka S, Kobayashi H*, et al.* Prognostic factors for survival in patients with high-grade meningioma and recurrence-risk stratification for application of radiotherapy. PLoS One 2014;9:e97108.

34. Abry E, Thomassen IO, Salvesen OO, Torp SH. The significance of Ki-67/MIB-1 labeling index in human meningiomas: a literature study. Pathol Res Pract 2010;206:810-5.

35. Goutagny S, Nault JC, Mallet M*, et al.* High incidence of activating TERT promoter mutations in meningiomas undergoing malignant progression. Brain Pathol 2014;24:184-9.

36. Sahm F, Schrimpf D, Olar A*, et al.* TERT Promoter Mutations and Risk of Recurrence in Meningioma. J Natl Cancer

Inst 2016;108.

37. Abedalthagafi M, Bi WL, Aizer AA*, et al.* Oncogenic PI3K mutations are as common as AKT1 and SMO mutations in meningioma. Neuro Oncol 2016. [Epub ahead of print]

38. Aboukais R, Baroncini M, Zairi F, Reyns N, Lejeune JP. Early postoperative radiotherapy improves progression free survival in patients with grade 2 meningioma. Acta Neurochir (Wien) 2013;155:1385-90.

39. Kaur G, Sayegh ET, Larson A*, et al.* Adjuvant radiotherapy for atypical and malignant meningiomas: a systematic review. Neuro Oncol 2014;16:628-36.

40. Han SW, Kim TY, Hwang PG*, et al.* Predictive and prognostic impact of epidermal growth factor receptor mutation in non-small-cell lung cancer patients treated with gefitinib. J Clin Oncol 2005;23:2493-501.

41. Plesec TP, Hunt JL. KRAS mutation testing in colorectal cancer. Adv Anat Pathol 2009;16:196-203.

42. Shepherd C, Puzanov I, Sosman JA. B-RAF inhibitors: an evolving role in the therapy of malignant melanoma. Curr Oncol Rep 2010;12:146-52.

43. Brastianos PK, Horowitz PM, Santagata S*, et al.* Genomic sequencing of meningiomas identifies oncogenic SMO and AKT1 mutations. Nat Genet 2013;45:285-9.

44. Staff S, Kujala P, Karhu R*, et al.* Preservation of nucleic acids and tissue morphology in paraffin-embedded clinical samples: comparison of five molecular fixatives. J Clin Pathol 2013;66:807-10.

45. Viertler C, Groelz D, Gundisch S*, et al.* A new technology for stabilization of biomolecules in tissues for combined histological and molecular analyses. J Mol Diagn 2012;14:458-66.

46. Kap M, Smedts F, Oosterhuis W*, et al.* Histological assessment of PAXgene tissue fixation and stabilization reagents. PLoS One 2011;6:e27704.

47. Howat WJ, Wilson BA. Tissue fixation and the effect of molecular fixatives on downstream staining procedures. Methods 2014;70:12-9.

48. Lehmann U, Kreipe H. Real-time PCR analysis of DNA and RNA extracted from formalin-fixed and paraffin-embedded biopsies. Methods 2001;25:409-18.

49. Nam SK, Im J, Kwak Y*, et al.* Effects of fixation and storage of human tissue samples on nucleic Acid preservation. Korean J Pathol 2014;48:36-42.

Titles and legends to figures

Figure 1 Genotype and clinicopathological findings.

Samples from patients were separated according to genotype. At the top of the figure, the clinical features are summarized. In the middle portion of the figure, copy number alterations and mutations are shown. At the bottom of the figure, the pathological findings are presented. FISH, fluorescent *in situ* hybridization; CNA, copy number alteration.

Figure 2 Genotype and clinical features.

A, The frequency of each gene alteration. The number indicates the number of cases carrying each gene alteration. B, Tumor location and genotype. Two cases of intraventricular meningioma were excluded. C, Tumor volume according to genotype. Newly diagnosed meningiomas were analyzed (n = 65). Box plots show the median (horizontal line), first to third quartiles of size (box) and 1.5 times the interquartile range (whiskers). D, Genotype and recurrence-free survival. Ninety cases of newly diagnosed and recurrent meningiomas were analyzed.

Figure 3 The scheme of the clinical sequencing system and treatment strategy for meningioma.

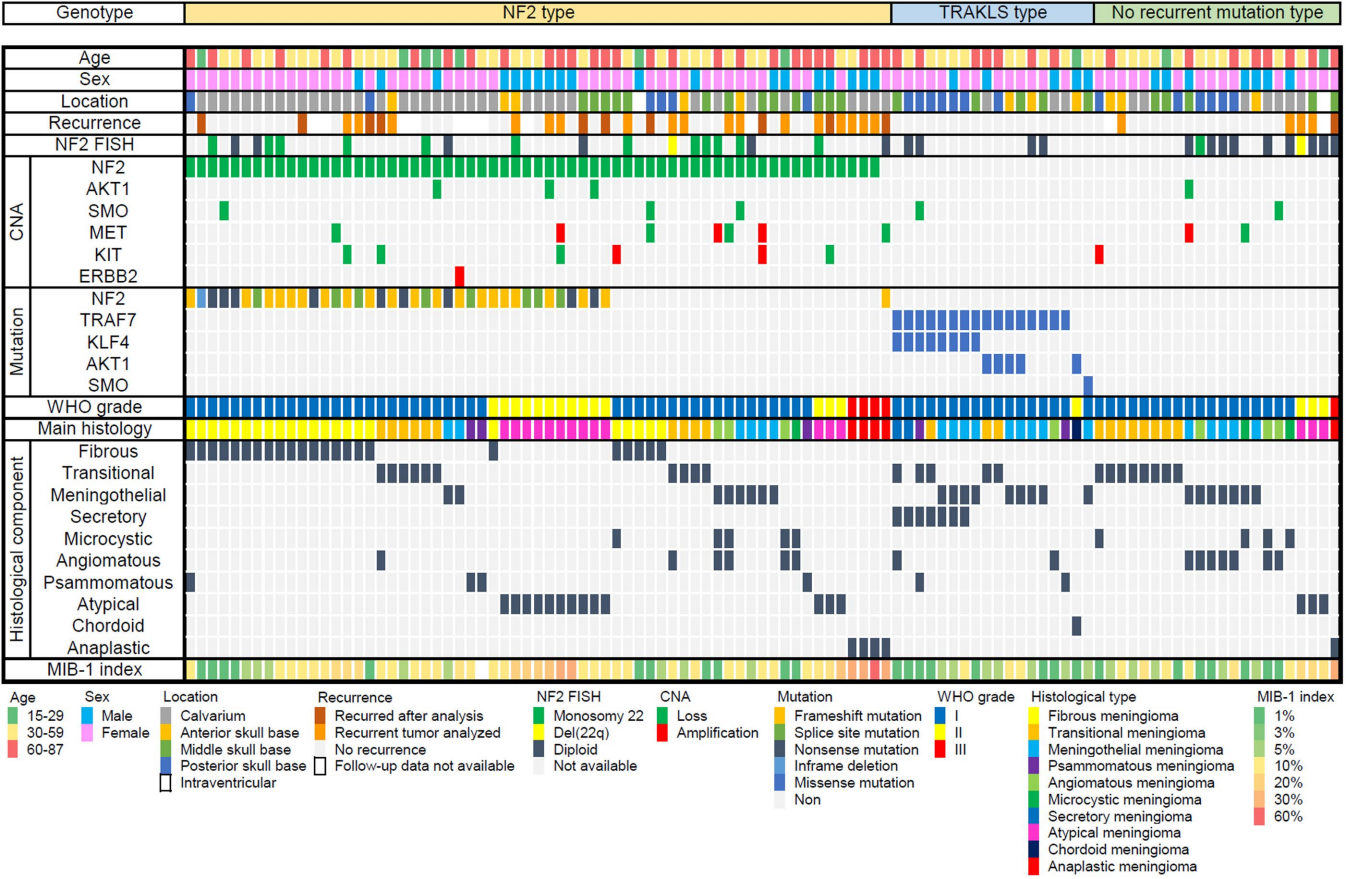
Genotype
NF2 type
TRAKLS type
No recurrent mutation type
Age
Sex
Location
Recurrence
NF2 FISH
CNA
NF2
AKT1
SMO
MET
KIT
ERBB2
Mutation
NF2
TRAF7
KLF4
AKT1
SMO
WHO grade
Main histology
Histological component
Fibrous
Transitional
Meningothelial
Secretory
Microcystic
Angiomatous
Psammomatous
Atypical
Chordoid
Anaplastic
MIB-1 index
Age
15-29
30-59
60-87
Sex
Male
Female
Location
Calvarium
Anterior skull base
Middle skull base
Posterior skull base
Intraventricular
Recurrence
Recurred after analysis
Recurrent tumor analyzed
No recurrence
Follow-up data not available
NF2 FISH
Monosomy 22
Del(22q)
Diploid
Not available
CNA
Loss
Amplification
Mutation
Frameshift mutation
Splice site mutation
Nonsense mutation
Inframe deletion
Missense mutation
Non
WHO grade
I
II
III
Histological type
Fibrous meningioma
Transitional meningioma
Meningothelial meningioma
Psammomatous meningioma
Angiomatous meningioma
Microcystic meningioma
Secretory meningioma
Atypical meningioma
Chordoid meningioma
Anaplastic meningioma
MIB-1 index
1%
3%
5%
10%
20%
30%
60%

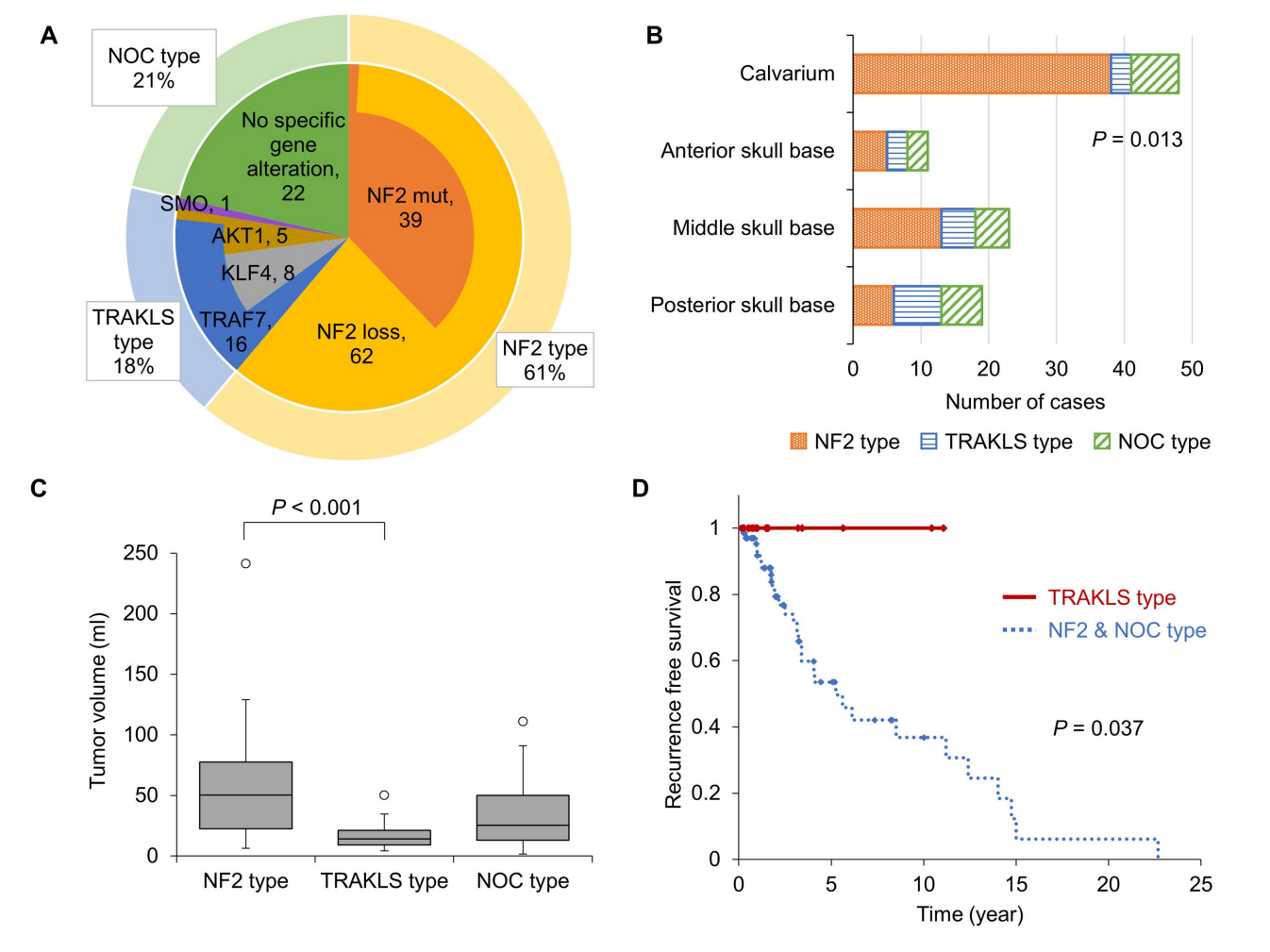
A
NOC type
21%
No specific
gene
alteration,
22
SMO, 1
AKT1, 5
KLF4, 8
TRAF7,
16
TRAKLS
type
18%
NF2 mut,
39
NF2 loss,
62
NF2 type
61%
B
Calvarium
Anterior skull base
Middle skull base
Posterior skull base
P = 0.013
0
10
20
30
40
50
Number of cases
NF2 type
TRAKLS type
NOC type
C
P < 0.001
Tumor volume (ml)
250
200
150
100
50
0
NF2 type
TRAKLS type
NOC type
D
Recurrence free survival
1
0.8
0.6
0.4
0.2
0
TRAKLS type
NF2 & NOC type
P = 0.037
0
5
10
15
20
25
Time (year)

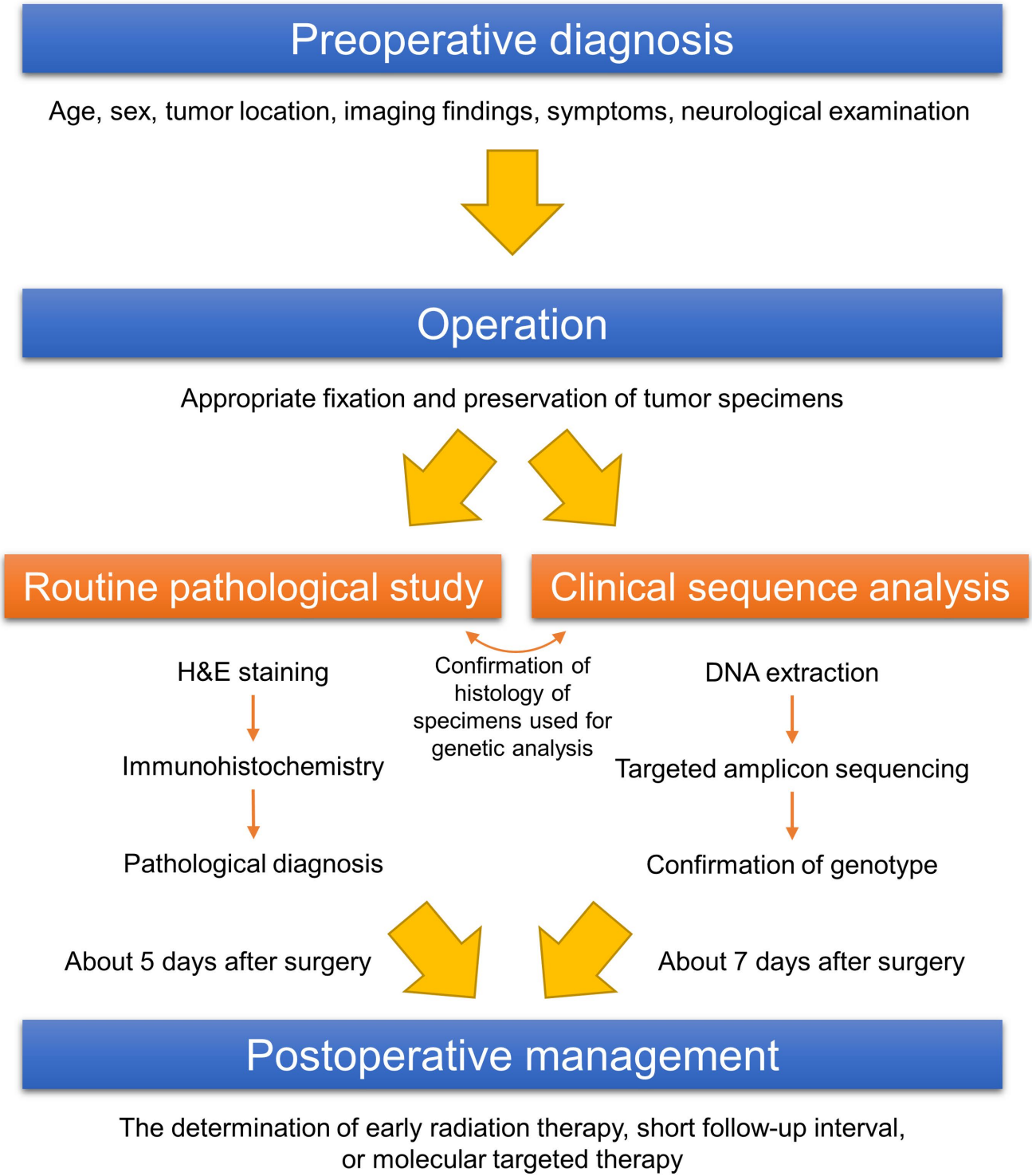
Preoperative diagnosis
Age, sex, tumor location, imaging findings, symptoms, neurological examination
Operation
Appropriate fixation and preservation of tumor specimens
Routine pathological study
Clinical sequence analysis
H&E staining
Immunohistochemistry
Pathological diagnosis
Confirmation of histology of specimens used for genetic analysis
DNA extraction
Targeted amplicon sequencing
Confirmation of genotype
About 5 days after surgery
About 7 days after surgery
Postoperative management
The determination of early radiation therapy, short follow-up interval, or molecular targeted therapy

Table 1. Clinicopathological features of patients according to genotype

Characteristics	Total (*n* = 103)	NF2 type (*n* = 63)	TRAKLS (*n* = 18)	NOC type (*n* = 22)
Sex – no. (%)				
Male	31 (30)	19 (30)	5 (28)	7 (32)
Female	72 (70)	44 (70)	13 (72)	15 (68)
Age – yr				
Median	55	57	56	50
Range	15–87	15–87	24–78	23–78
Tumor location – no. (%)				
Calvarium	48 (47)	38 (60)	3 (17)	7 (32)
Anterior skull base	11 (11)	5 (8)	3 (17)	3 (14)
Middle skull base	23 (22)	13 (21)	5 (28)	5 (23)
Posterior skull base	19 (18)	6 (10)	7 (39)	6 (27)
Intraventricular	2 (2)	1 (2)	0 (0)	1 (5)
Diagnosis – no. (%)				
WHO grade I	80 (78)	45 (71)	17 (94)	18 (82)
Fibrous meningioma	22 (21)	22 (35)	0 (0)	0 (0)
Transitional meningioma	21 (20)	10 (16)	3 (17)	8 (36)
Meningothelial meningioma	20 (19)	6 (10)	9 (50)	5 (23)
Angiomatous meningioma	7 (7)	3 (5)	1 (6)	3 (14)
Psammomatous meningioma	5 (5)	3 (5)	2 (11)	0 (0)
Microcystic meningioma	3 (3)	1 (2)	0 (0)	2 (9)
Secretory meningioma	2 (2)	0 (0)	2 (11)	0 (0)
WHO grade II	18 (17)	14 (22)	1 (6)	3 (14)
Atypical meningioma	16 (16)	13 (21)	0 (0)	3 (14)
Fibrous meningioma with brain invasion	1 (1)	1 (2)	0 (0)	0 (0)
Chordoid meningioma	1 (1)	0 (0)	1 (6)	0 (0)
WHO grade III	5 (5)	4 (6)	0 (0)	1 (5)
Anaplastic meningioma	5 (5)	4 (6)	0 (0)	1 (5)

Table 2. Imaging characteristics according to genotype

	NF2 type (*n* = 36)	**TRAKLS type (*n* = 18)**	**NOC type (*n* = 18)**	***P* value**
Calcification	15/36 (42%)	5/18 (28%)	0/18 (0%)	**0.006**
Adjacent bone change [a]	17/30 (57%)	2/17 (12%)	2/15 (13%)	**0.001**
Peritumoral cyst	4/36 (11%)	0/18 (0%)	3/18 (17%)	0.222
Peritumoral edema	24/36 (67%)	9/18 (50%)	7/18 (39%)	0.132
Heterogeneous gadolinium enhancement	16/36 (44%)	0/18 (0%)	3/18 (17%)	**0.001**

Preoperative imaging data of newly diagnosed meningioma were analyzed.

[a] Excluded falx, tentorial and intraventricular meningioma owing to no or less attachment with bone.

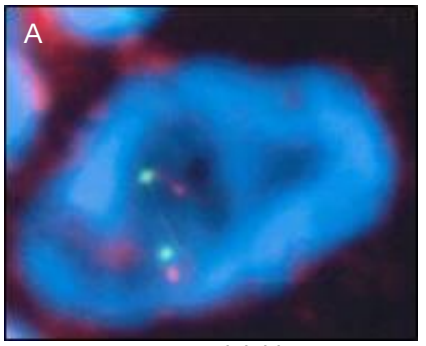

T524: Diploid
(NGS score *Q* = 48)

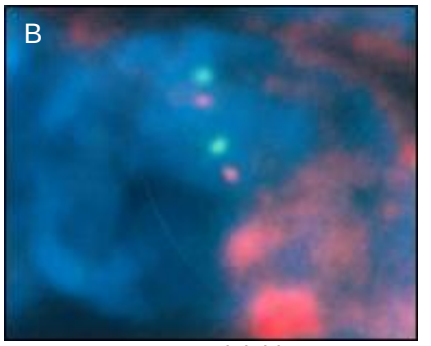

T750: Diploid
(NGS score *Q* = 58)

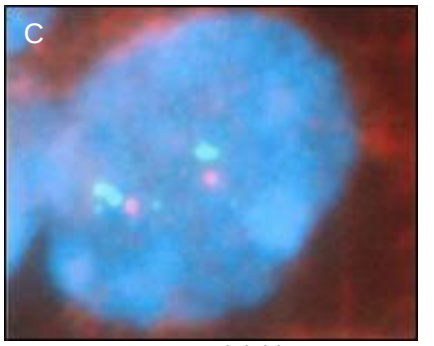

T369: Diploid
(NGS score *Q* = 144)

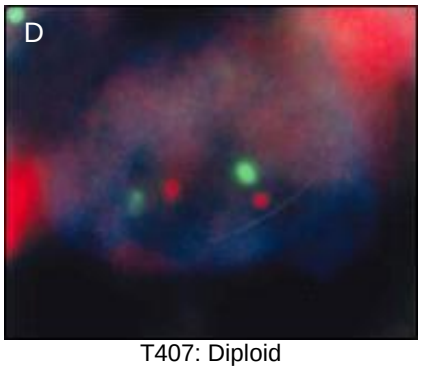

T407: Diploid
(NGS score *Q* = 205)

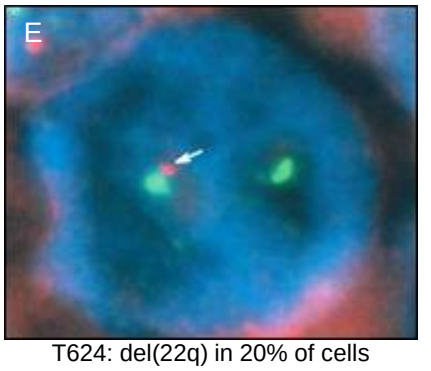

T624: del(22q) in 20% of cells
(NGS score *Q* = 2)

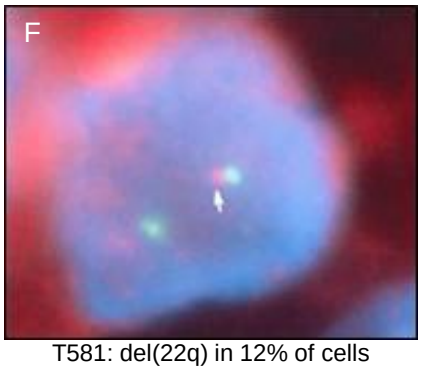

T581: del(22q) in 12% of cells
(NGS score *Q* = 170)

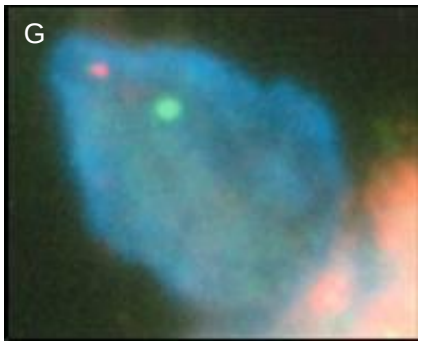

T629: Monosomy in 100% of cells
(NGS score *Q* = 124)

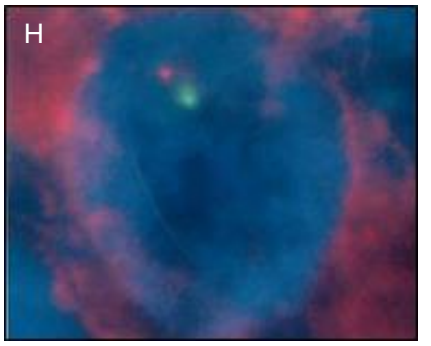

T693: Monosomy in 68% of cells
(NGS score *Q* = 236)

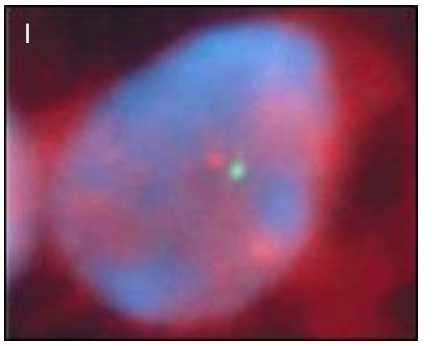

T571: Monosomy in 100% of cells
(NGS score *Q* = 250)

J. T799

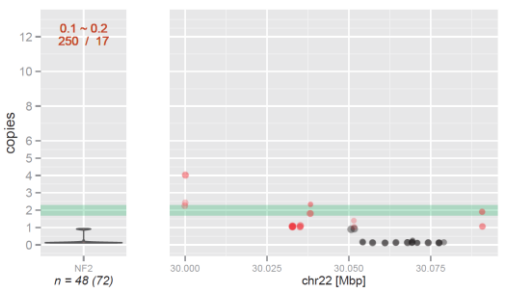

NF2 mutation: No
FISH: unanalyzable

K. T243

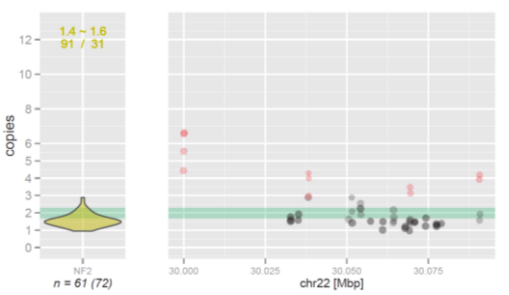

NF2 mutation: No
FISH: diploid (0%)

L. T839

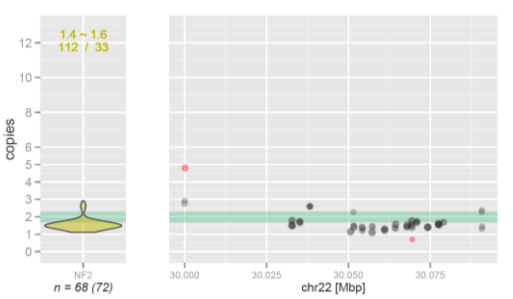

NF2 mutation: p.Gln65*/c.193C>T
FISH: diploid (0%)

M. T624

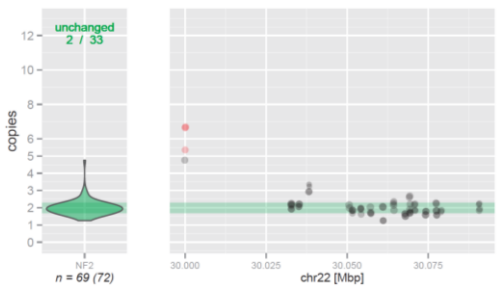

NF2 mutation: No
FISH: del(22q) (20%)

N. T798

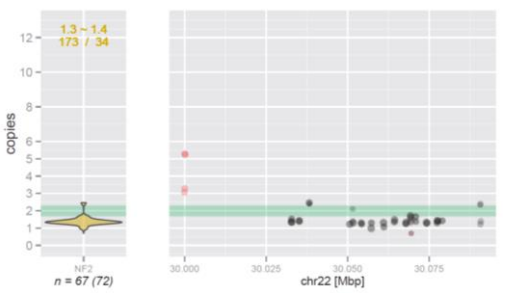

NF2 mutation: p.Arg198*/c.592C>T
FISH: diploid (0%)

O. T407

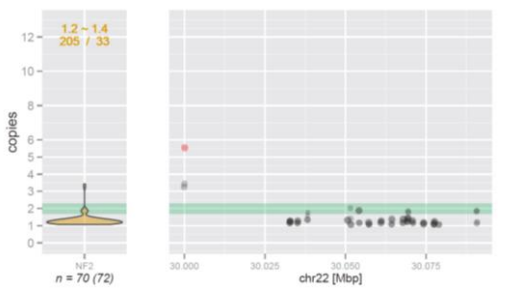

NF2 mutation:
c.364_381delTCTCCCTTGTTGCTCCTT
FISH: diploid (0%)

P. T771

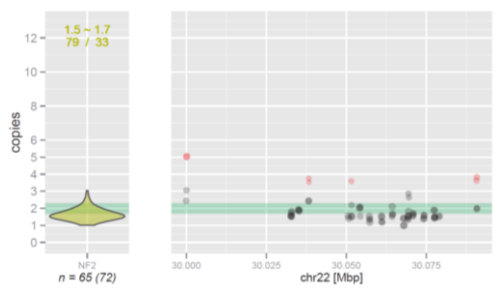

NF2 mutation: No
FISH: monosomy (60%)

Q. T603

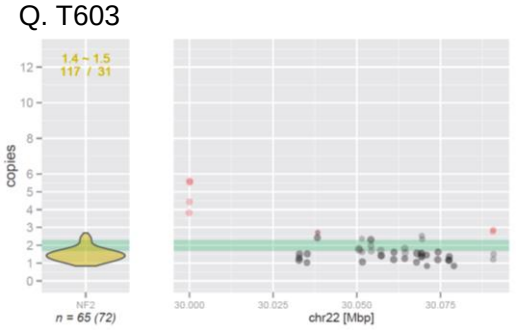

NF2 mutation:
p.Cys133_Pro134fs/c.399_400insC
FISH: monosomy (68%)

R. T690

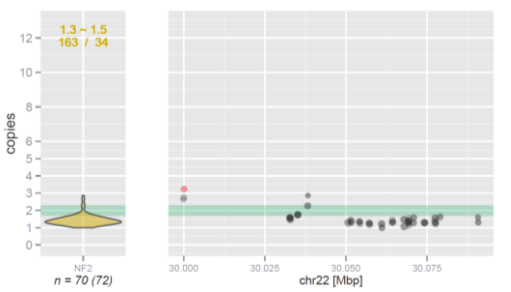

NF2 mutation:
p.Arg447fs/c.1341_1345delGCAGG
FISH: monosomy (81%)

Supplementary Figure 1. Results of (**A–I**) fluorescent *in situ* hybridization (FISH) and (**J–R**) copy number alteration analysis by next-generation sequencing (NGS) of representative cases. **A–D** showed diploid karyotype, **E** and **F** displayed del(22q), and **G–I** showed monosomy 22. Green: Centromere of chromosome 22, red: NF2. **J** showed biallelic loss of NF2. **K**–**O** displayed discordant results between NGS analysis and FISH and **P**–**R** showed concordant results.

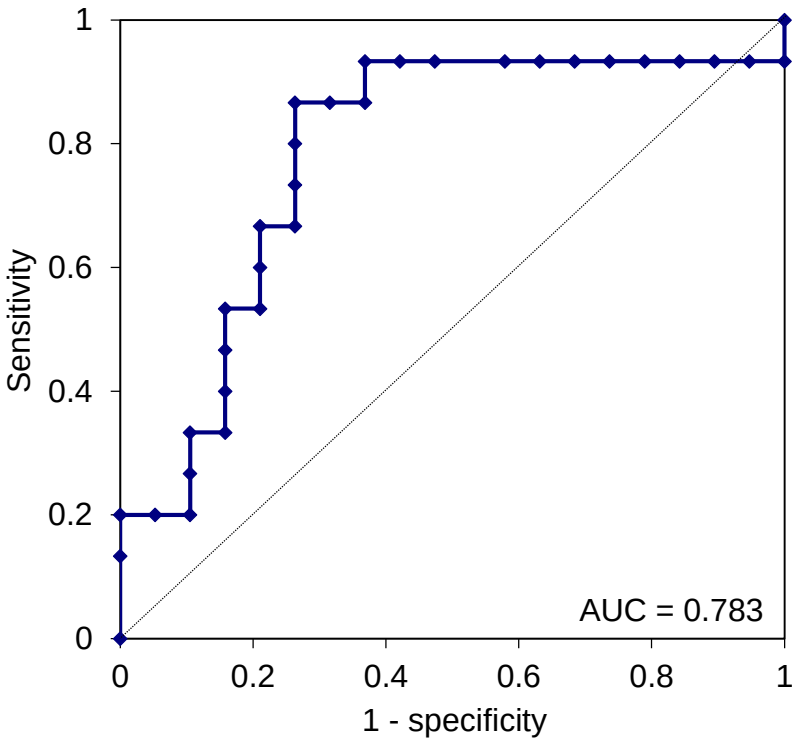

Supplementary Figure 2. The receiver operating characteristic curve for next-generation sequencing against interphase-fluorescent *in situ* hybridization. The score *Q* = 79 presented maximum Youden index with sensitivity and specificity as 86.7% and 73.7%, respectively. AUC, the area under the curve.

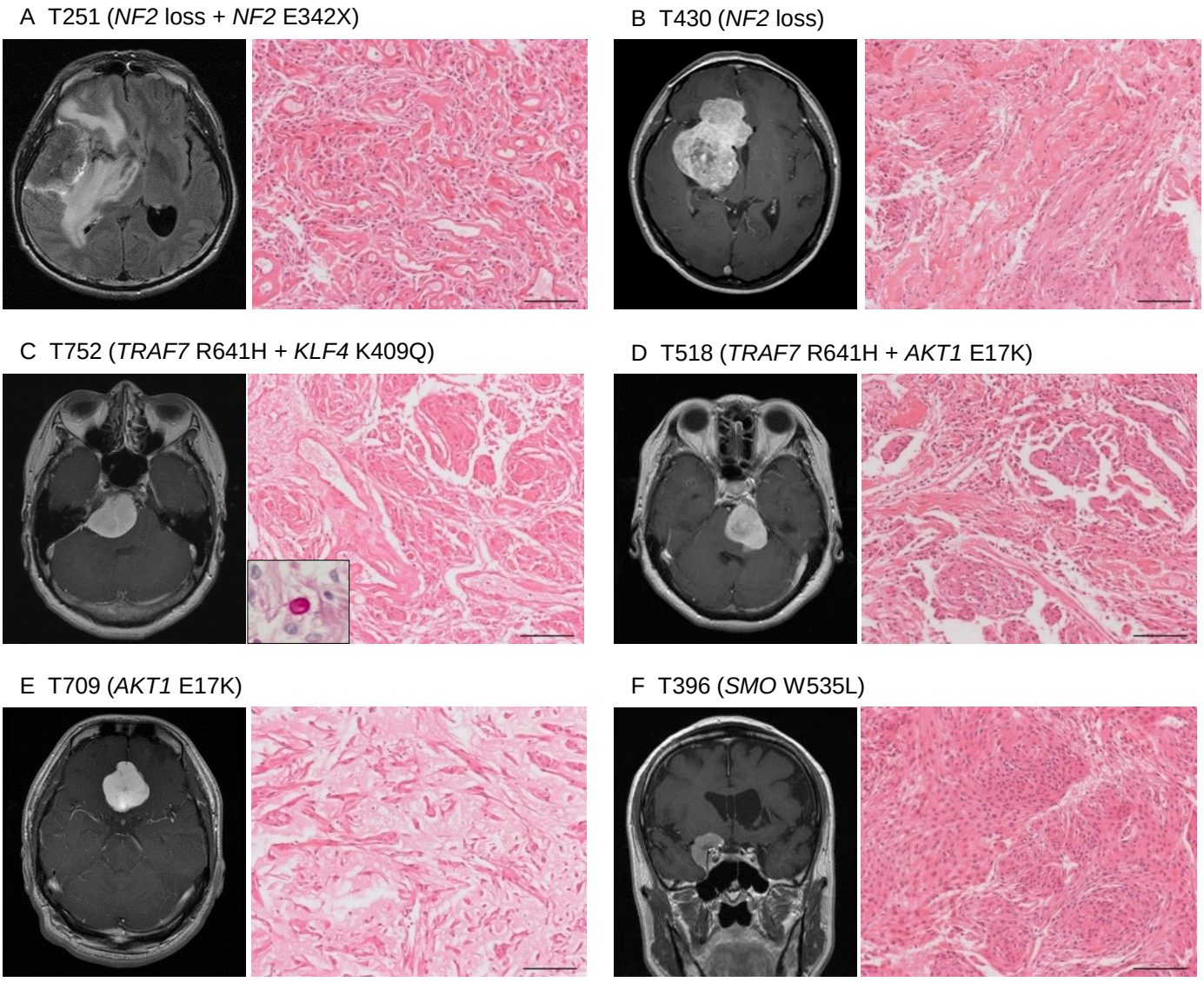

Supplementary Figure 3. Magnetic resonance imaging (MRI) and hematoxylin and eosin (H&E) staining of representative cases. Insert of **C**: Periodic acid-Schiff (PAS) staining. *NF2* status of **A** and **B** is based on next-generation sequencing. Scale bar: 100 µm.

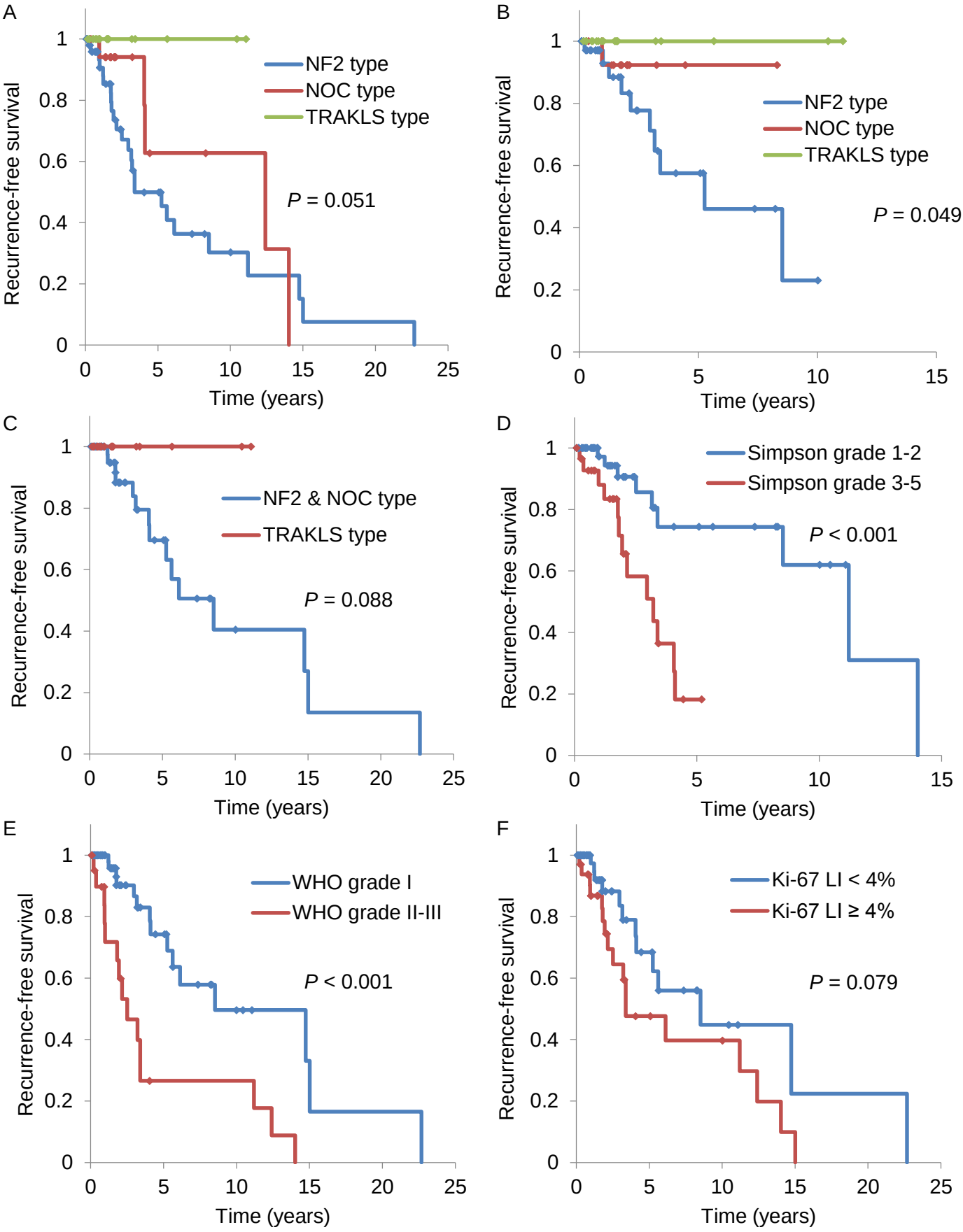

Supplementary Figure 4. Recurrence-free survival according to **A-C** genotype, **D** Simpson grade, **E** WHO grade, and **F** Ki-67 labeling index (LI). **C**, Only WHO grade I cases are included. Newly diagnosed and recurrent meningiomas were included in **A**, **C**, **D**, **E** and **F**, and only newly diagnosed meningiomas were analyzed in **B**.

Supplementary Table 1 Clinicopathological features

Tumor ID	Primary/ Recurrent tumor	Sex	Age	Primary lesion	Primary lesion detail	Neurofibromatosis type 2	Radiotherapy	Tumor volume (ml)	Peritumoral edema	Peritumoral cyst	Calcification	Bone change	Gadolinium enhancement	Simpson Grade	Recurrence	Recurrence free survival (months)	Survival	Overall survival (months)	WHO grade	Histology	Other histological component	Ki-67 Labeling Index
T252	primary	Female	66	calvarium	lt frontal falx									4	yes	2.5	dead	5.9	III	Anaplastic meningioma		30%
T630	recurrent	Female	51	middle fossa	cavernous sinus		RT-induced							4	yes	14.6	alive	87.2	I	Angiomatous meningioma	Meningothelial/Microcystic	3%
T760	primary	Male	23	calvarium	convexity		RT-induced	241.3	yes	no	no	no	heterogenous	4	no	9.9	alive	9.9	I	Transitional meningioma		5%
T764	primary	Female	44	anterior fossa	olfactory groove			11.8	yes	no	no	no	homogenous	2	no	12.0	alive	12.0	I	Meningothelial meningioma		5%
T138	primary	Male	60	calvarium	frontal convexity			22.6	yes	no	no	no	homogenous	2	no	132.8	alive	132.8	I	Angiomatous meningioma		1%
T275	primary	Female	29	calvarium	parietal convexity			27.1	yes	no	no	yes	heterogenous	1	no	60.9	alive	60.9	I	Transitional meningioma		5%
T679	primary	Female	36	posterior fossa	petrosal			4.3	no	no	no	no	homogenous	2	no	17.7	alive	17.7	I	Meningothelial meningioma	Secretory	4%
T682	primary	Male	62	calvarium	frontal falx meningioma			25.3	yes	no	no	N/A	heterogenous	2	no	21.2	alive	21.2	I	Angiomatous meningioma	Microcystic	1%
T691	primary	Female	62	anterior fossa	tuberculum sellae			12.8	no	no	no	no	homogenous		N/A		N/A		I	Transitional meningioma		2%
T700	primary	Female	71	middle fossa	cavernous-temporal fossa-petrosal			50.1	yes	no	no	no	homogenous	4	no	19.2	alive	19.2	I	Secretory meningioma	Transitional/Angiomatous	1%
T709	primary	Male	24	anterior fossa	planum sphenoidale			19.4	no	no	no	no	homogenous	2	no	11.1	alive	11.1	II	Chordoid meningioma		1%
T752	primary	Female	54	posterior fossa	petroclival			24.4	no	no	no	no	homogenous	3	no	9.5	alive	9.5	I	Meningothelial meningioma	Secretory	2%
T753	primary	Male	67	middle fossa	sphenoid ridge - middle fossa - intraorbital			53.9	no	no	yes	yes	homogenous	2	no	11.9	alive	11.9	I	Meningothelial meningioma		4%
T758	primary	Female	69	posterior fossa	petroclival			50	no	no	no	no	homogenous	4	no	17.2	alive	17.2	I	Meningothelial meningioma	Angiomatous	7%
T766	primary	Female	72	calvarium	parietal convexity										N/A		N/A		I	Fibrous meningioma		5%
T31	primary	Female	16	calvarium	frontal convexity										N/A		N/A		I	Meningothelial meningioma	With atypical foci	7%
T65	primary	Female	15	calvarium	parasagittal	yes			N/A	no	no	no	homogenous		N/A		N/A		I	Transitional meningioma		2%
T87	primary	Female	69	calvarium	falx			79.5	no	yes	no	N/A	heterogenous	1	no	98.7	alive	98.7	I	Fibrous meningioma		2%
T91	primary	Female	55	calvarium	frontal convexity			11.3	no	no	no	yes	homogenous	1	no	120.1	alive	120.1	I	Fibrous meningioma		10%
T192	recurrent	Female	77	calvarium	lt frontal convexity										yes	73.5	dead	103.3	I	Fibrous meningioma		10%
T208	primary	Female	60	middle fossa	sphenoid ridge			45.3	yes	no	no	yes	heterogenous	2	no	5.9	alive	5.9	I	Microcystic meningioma	Angiomatous	1%
T237	recurrent	Male	48	calvarium	lt frontal, parasagittal									2	yes	21.1	alive	147.2	I	Fibrous meningioma		10%
T243	primary	Female	43	calvarium	lt occipital										N/A		N/A		I	Meningothelial meningioma		2%
T321	primary	Male	38	calvarium	frontal convexity										N/A		N/A		II	Atypical meningioma		15%
T325	recurrent	Male	76	calvarium	parasagittal, posterior third									3	yes	23.3	dead	76.2	II	Atypical meningioma		30%
T369	primary	Female	43	middle fossa	rt. temporal sphenoid ridge, nasal cavity, anterior skull base			108.9	yes	no	no	yes	homogenous	3	yes	11.8	alive	74.7	II	Atypical meningioma		3%
T387	primary	Female	74	middle fossa	lt temporal, sphenoid ridge			20.2	yes	no	yes	yes	homogenous	2	yes	40.7	alive	67.5	II	Atypical meningioma		4%
T398	primary	Female	65	calvarium	rt parietal convexity										N/A		N/A		I	Psammomatous meningioma		5%
T409	recurrent	Female	78	middle fossa	clinoidal & convexity		unknown								yes	148.9	alive	237.6	II	Atypical meningioma		10%
T413	primary	Female	20	calvarium	rt fronto-parietal giant convexity			129	no	no	yes	yes	homogenous	2	yes	37.9	alive	61.3	I	Fibrous meningioma		1%
T415	recurrent	Female	57	anterior fossa	orbital										yes	67.4	alive	131.3	I	Transitional meningioma		3%
T430	primary	Female	61	posterior fossa	posterior clinoid			107	yes	no	no	no	heterogenous	2	yes	14.8	alive	58.4	I	Fibrous meningioma		1%
T466	recurrent	Male	72	calvarium	rt parietal parasagittal		post-RT							4	yes	4.4	dead	22.6	III	Anaplastic meningioma		60%
T482	primary	Male	28	others	intraventricle			88.2	yes	yes	yes	N/A	heterogenous	2	no	16.9	alive	16.9	I	Fibrous meningioma		1%
T496	recurrent	Male	52	anterior fossa	lt orbital		post-RT							4	yes	21.7	dead	79.9	II	Atypical meningioma		15%
T571	recurrent	Female	59	middle fossa	lt cavernous sinus		post-RT								yes	180.1	dead	221.6	I	Fibrous meningioma		4%
T580	primary	Male	55	calvarium	falx middle third			87.1	yes	no	no	N/A	homogenous	1	no	39.4	alive	39.4	I	Transitional meningioma		5%
T621	primary	Male	65	middle fossa	sphenoid ridge inner third			111	no	yes	no	no	heterogenous	4	no	25.1	alive	25.1	I	Meningothelial meningioma	Angiomatous	4%
T623	primary	Female	35	calvarium	frontal convexity			67.3	yes	yes	no	yes	homogenous	1	no	24.3	alive	24.3	I	Transitional meningioma		7%
T624	recurrent	Female	45	calvarium	rt cerebellar, tentorial									1	yes	168.3	alive	206.5	II	Atypical meningioma		10%
T650	primary	Female	57	calvarium	temporal convexity			6.5	yes	yes	no	yes	homogenous	1	no	24.9	alive	24.9	II	Fibrous meningioma with brain invasion		4%
T651	primary	Male	73	middle fossa	cavernous sinus			75.1	yes	no	no	yes	heterogenous	4	yes	25.8	dead	25.8	II	Atypical meningioma		7%
T690	primary	Female	66	calvarium	frontal convexity			14.9	no	no	yes	yes	homogenous	1	no	20.8	alive	20.8	I	Fibrous meningioma		3%
T693	recurrent	Male	70	middle fossa	temporal base		post-RT							1	yes	134.4	alive	292.1	II	Atypical meningioma		5%
T666	primary	Male	49	posterior fossa	petroclival			14.2	no	no	no	no	homogenous	2	no	8.6	alive	8.6	I	Meningothelial meningioma	Secretory	2%
T779	recurrent	Male	52	calvarium	lt parasagittal anterior third		post-RT							4	yes	40.7	dead	172.1	III	Anaplastic meningioma		30%
T799	recurrent	Male	71	calvarium	rt middle third parasagittal		post-RT								yes	11.2	N/A	54.5	III	Anaplastic meningioma		30%
T399	primary	Female	67	middle fossa	lt temporal. sphenoid ridge outer third			44.2	yes	no	no	no	heterogenous	2	yes	11.4	dead	40.1	III	Anaplastic meningioma		30%
T1167	primary	Male	62	calvarium	rt fronto-parietal, convexity				no	no	no	no	heterogenous	1	no	48.6	alive	48.6	II	Atypical meningioma		30%
T684	recurrent	Male	87	calvarium	lt parietal, convexity									2	yes	30.1	alive	45.0	II	Atypical meningioma		20%
T780	primary	Male	41	calvarium	parasagittal				yes	no	yes	yes	heterogenous	2	no	9.2	alive	9.2	II	Atypical meningioma		15%
T54	primary	Female	49	calvarium	lt fronto-parietal convexity			9.9	no	no	no	no	heterogenous	1	no	19.8	alive	19.8	I	Fibrous meningioma		3%
T133	recurrent	Female	43	anterior fossa	intraorbital (optic nerve sheath)		post-RT								yes	176.9	alive	310.1	I	Transitional meningioma		2%
T251	primary	Male	56	calvarium	temporal convexity			75.4	yes	no	no	no	heterogenous	1	yes	102.2	alive	103.8	I	Transitional meningioma	Angiomatous	3%
T253	primary	Female	34	calvarium	parietal convexity			17	no	yes	no	no	homogenous	1	no	99.6	alive	99.6	I	Angiomatous meningioma		1%
T256	primary	Female	69	calvarium	parasagittal/frontal			15.5	yes	no	no	no	homogenous	2	no	88.3	alive	88.3	I	Angiomatous meningioma	Microcystic/Meningothelial	1%
T286	recurrent	Female	38	anterior fossa	tuberculum sellae									3	yes	48.7	alive	88.2	I	Transitional meningioma		3%
T293	recurrent	Male	71	calvarium	parasagittal									3	yes	49.2	alive	125.2	I	Microcystic meningioma		3%
T396	primary	Male	57	middle fossa	paraclinoidal			5.4	no	no	yes	no	homogenous	2	no	67.7	alive	67.7	I	Meningothelial meningioma		2%
T407	primary	Female	59	calvarium	lt frontal parasagittal			25	yes	no	no	yes	homogenous	3	no	62.3	alive	62.3	I	Fibrous meningioma		2%
T461	primary	Female	55	posterior fossa	Petroclival			16.9	yes	no	no	no	homogenous	3	no	53.3	alive	53.3	I	Meningothelial meningioma	Angiomatous	2%
T467	primary	Female	55	posterior fossa	posterior fossa petrosal			46.3	yes	no	yes	no	heterogenous	3	yes	35.5	alive	55.8	I	Fibrous meningioma		1%
T500	primary	Female	23	others	lt insular intraparenchymal		RT-induced	62.9	yes	no	no	N/A	homogenous		N/A		N/A		II	Atypical meningioma		7%
T517	primary	Female	38	posterior fossa	petrosal			36	yes	no	yes	yes	homogenous	2	no	1.0	alive	1.0	I	Fibrous meningioma		2%
T518	primary	Female	63	posterior fossa	petroclival			19.4	no	no	yes	no	homogenous	3	no	41.1	alive	41.1	I	Transitional meningioma		2%
T524	primary	Female	74	anterior fossa	olfactory gloove			5.3	yes	no	no	yes	homogenous	2	no	38.4	alive	38.4	I	Meningothelial meningioma		2%
T559	primary	Female	48	middle fossa	clinoid			37.4	yes	no	no	yes	homogenous	4	yes	21.2	alive	38.2	I	Meningothelial meningioma		3%
T581	recurrent	Female	78	posterior fossa	petroclival									4	N/A		N/A		I	Transitional meningioma	Angiomatous	3%
T603	primary	Female	53	calvarium	frontal falx			9	no	no	yes	N/A	homogenous	2	no	28.7	alive	28.7	I	Fibrous meningioma		2%
T612	primary	Male	29	middle fossa	sphenoid ridge inner third			91	no	no	no	no	homogenous	2	no	38.8	alive	38.8	I	Transitional meningioma		4%
T629	primary	Female	61	calvarium	falx posterior third			54.9	no	no	yes	N/A	heterogenous	1	no	29.3	alive	29.3	I	Fibrous meningioma		1%
T642	primary	Female	35	posterior fossa	petroclival			45.7	no	no	no	no	homogenous	3	no	24.0	alive	24.0	I	Transitional meningioma		1%
T657	primary	Male	60	anterior fossa	planum sphenoidale			6.4	no	no	no	no	homogenous	2	no	11.3	alive	11.3	I	Meningothelial meningioma		2%
T661	primary	Female	51	posterior fossa	petrosal			13.1	no	no	no	no	homogenous	2	no	23.8	alive	23.8	I	Angiomatous meningioma	Meningothelial	1%
T674	primary	Male	39	middle fossa	cavernous sinus			15.9	no	no	no	no	homogenous	4	no	20.5	alive	20.5	I	Transitional meningioma		2%
T686	primary	Female	56	posterior fossa	petrosal			1.8	no	no	no	yes	homogenous	2	no	21.1	alive	21.1	I	Transitional meningioma	Microcystic	1%
T688	primary	Female	78	middle fossa	sphenoid ridge (inner third)			9.2	no	no	no	no	homogenous	4	no	18.7	alive	18.7	I	Meningothelial meningioma		1%
T699	primary	Male	48	calvarium	parasagittal				yes	no	no	no	homogenous	2	no	16.3	alive	16.3	I	Microcystic meningioma	Meningothelial	1%
T717	primary	Female	53	posterior fossa	petroclival			34.7	yes	no	no	no	homogenous	4	no	3.3	alive	3.3	I	Secretory meningioma		1%
T744	primary	Female	41	middle fossa	anterior clinoid			11.4	yes	no	no	no	homogenous	4	no	3.4	alive	3.4	I	Meningothelial meningioma		3%
T750	primary	Female	46	posterior fossa	petrosal			41.6	yes	no	no	no	homogenous	2	no	4.5	alive	4.5	I	Meningothelial meningioma	Angiomatous	1%
T771	recurrent	Female	63	anterior fossa	tuberculum sellae										yes	272.1	alive	279.6	I	Meningothelial meningioma		3%
T775	primary	Female	72	posterior fossa	Petroclival			7.3	yes	no	no	no	homogenous	4	no	6.7	alive	6.7	I	Psammomatous meningioma	Transitional/Secretory	1%
T777	recurrent	Female	52	middle fossa	cavernous sinus		post-RT							5	yes	38.6	alive	48.4	II	Atypical meningioma		20%
T782	primary	Female	67	posterior fossa	posterior fossa convexity			44.4	yes	no	yes	yes	homogenous	2	no	5.3	alive	5.3	I	Fibrous meningioma	Psammomatous	3%
T783	primary	Female	55	calvarium	falx				yes	no	no	N/A	heterogenous	1	no	9.9	alive	9.9	I	Fibrous meningioma		1%
T789	primary	Female	63	posterior fossa	petrosal			66.2	yes	no	yes	yes	homogenous	3	no	8.2	alive	8.2	I	Psammomatous meningioma		3%
T792	primary	Female	52	middle fossa	anterior clinoid			50.3	yes	no	no	no	homogenous	2	no	9.3	alive	9.3	I	Transitional meningioma		1%
T795	primary	Female	53	calvarium	falx										N/A		N/A		I	Psammomatous meningioma		N/A
T798	primary	Female	67	calvarium	convexity			9.7	no	no	no	no	homogenous	2	no	8.0	alive	8.0	I	Meningothelial meningioma		2%
T808	primary	Female	34	calvarium	parasagittal										yes	63.0	N/A		I	Fibrous meningioma		3%
T809	primary	Male	61	calvarium	convexity			13.7	no	no	yes	no	homogenous	1	no	6.1	alive	6.1	I	Transitional meningioma		2%
T823	primary	Female	83	calvarium	convexity										N/A		N/A		I	Transitional meningioma		3%
T850	primary	Female	51	calvarium	falx										N/A		N/A		I	Fibrous meningioma		4%
T941	recurrent	Male	24	calvarium	falx		unknown								N/A		N/A		I	Angiomatous meningioma	Microcystic	1%
T1520	primary	Female	52	middle fossa	frontal-temporal base				yes	no	yes	yes	homogenous	1	no	125.3	alive	125.3	I	Meningothelial meningioma		1%
T1725	primary	Female	44	calvarium	tentorial			21.2	yes	no	yes	N/A	homogenous	2	no	18.3	alive	18.3	I	Psammomatous meningioma		2%
T826	primary	Female	57	posterior fossa	clivus			17.1	no	no	no	no	homogenous	2	no	2.0	alive	2.0	I	Transitional meningioma	Secretory	1%
T828	primary	Male	70	anterior fossa	anterior fossa, sphenoid ridge			95	yes	no	yes	no	heterogenous	4	no	3.2	alive	3.2	II	Atypical meningioma		5%
T829	primary	Female	66	middle fossa	sphenoid ridge			55.8	yes	yes	no	yes	heterogenous	2	no	3.7	alive	3.7	I	Fibrous meningioma	Microcystic	4%
T830	primary	Female	39	calvarium	tentorial			11.6	no	no	no	N/A	homogenous	2	no	3.5	alive	3.5	I	Transitional meningioma		2%
T834	primary	Female	79	middle fossa	middle fossa			66	yes	no	yes	no	homogenous	4	no	1.0	alive	1.0	II	Atypical meningioma		3%
T839	primary	Female	37	calvarium	convexity	yes			no	no	yes	no	homogenous	1	no	2.0	alive		I	Fibrous meningioma		1%

Supplementary Table 2 Copy number alterations of NF2 by next-generation sequencing (NGS) and fluorescent *in situ* hybridization (FISH), and copy number alterations of other genes by NGS

Tumor ID	NF2						Others										
	NGS score *Q*	NGS score *P*	NGS copy number min	NGS copy number max	FISH loss	FISH status	Gene name	Score *Q*	Score *P*	Copy number min	Copy number max	Gain/Loss	Gene name	Score *Q*	Score *P*	Copy number min	Copy number max	Gain/Loss
T252	30	30	1.6	1.9	0%	Diploid	MET	129	33	1.5	1.6	Loss						
T630	226	30	1.1	1.3			MET	123	32	1.5	1.6	Loss						
T760	240	30	1.1	1.2			AKT1	102	26	1.1	1.4	Loss						
T764	16	31	unchanged	unchanged														
T138	28	32	1.7	1.9														
T275	127	30	1.3	1.5	92%	Monosomy												
T679	38	29	1.6	1.8														
T682	78	32	1.5	1.7	0%	Diploid												
T691	25	31	unchanged	unchanged														
T700	34	31	1.6	1.8														
T709	6	31	unchanged	unchanged														
T752	36	31	1.6	1.8														
T753	250	31	0.9	1														
T758	56	29	1.5	1.7	0%	Diploid												
T766	249	31	1.1	1.2														
T31	250	32	1	1.2			ERBB2	112	34	2.4	2.6	Gain						
T65	198	32	1.2	1.3														
T87	250	32	1.1	1.2														
T91	199	32	1.2	1.3			MET	83	33	1.6	1.7	Loss						
T192	250	32	1.1	1.2	80%	Monosomy	KIT	200	31	1.2	1.4	Loss						
T208	222	32	1.2	1.3														
T237	214	27	1	1.3														
T243	91	31	1.4	1.6	0%	Diploid												
T321	244	30	1.1	1.2														
T325	245	29	1	1.2			KIT	107	31	1.4	1.6	Loss	MET	122	32	2.5	2.8	Gain
T369	144	31	1.3	1.5	0%	Diploid												
T387	216	30	1.1	1.3														
T398	250	30	1	1.1														
T409	71	32	1.5	1.7	0%	Diploid												
T413	250	31	1.1	1.2														
T415	203	31	1.2	1.3														
T430	180	32	1.2	1.4			MET	112	34	1.5	1.7	Loss	SMO	137	31	1.3	1.5	Loss
T466	250	32	1	1.1														
T482	242	32	1.1	1.2														
T496	99	27	1.3	1.5	86%	Monosomy												
T571	250	29	1	1.2	100%	Monosomy												
T580	93	27	1.3	1.6	65%	Monosomy												
T621	44	35	1.7	1.8	0%	Diploid	MET	90	36	2.3	2.5	Gain	AKT1	159	32	1.1	1.2	Loss
T623	13	32	unchanged	unchanged														
T624	2	33	unchanged	unchanged	20%	del(22q)												
T650	250	34	1.1	1.2														
T651	250	33	1.1	1.2			KIT	230	35	1.2	1.3	Loss						
T690	163	34	1.3	1.5	81%	Monosomy												
T693	236	32	1.1	1.3	68%	Monosomy												
T666	6	34	unchanged	unchanged														
T779	206	33	1.2	1.3														
T799	250	17	0.1	0.2														
T399	19	33	unchanged	unchanged	0%	Diploid												
T1167	178	33	1.3	1.4														
T684	250	33	1	1.1			AKT1	139	29	1.1	1.3	Loss						
T780	248	34	1.1	1.3														
T54	234	33	1.2	1.3														
T133	157	33	1.3	1.5														
T251	219	32	1..2	1.3			KIT	104	33	1.5	1.6	Loss						
T253	8	32	unchanged	unchanged			SMO	92	32	1.4	1.6	Loss						
T256	84	32	1.5	1.7	60%	Monosomy	MET	95	35	2.3	2.5	Gain						
T286	8	33	unchanged	unchanged														
T293	52	32	1.6	1.8	0%	Diploid												
T396	8	33	unchanged	unchanged														
T407	205	33	1.5	1.4	0%	Diploid												
T461	34	31	1.7	1.9	0%	Diploid												
T467	211	34	1.2	1.3														
T500	38	29	1.5	1.8	0%	Diploid												
T517	250	30	1	1.2														
T518	24	33	unchanged	unchanged														
T524	48	33	1.6	1.8	0%	Diploid												
T559	228	33	1.2	1.3			KIT	107	32	2.5	2.7	Gain	MET	105	36	2.3	2.5	Gain
T581	170	33	1.3	1.4	12%	del(22q)												
T603	117	31	1.4	1.5	68%	Monosomy												
T612	14	33	unchanged	unchanged														
T629	124	34	1.4	1.6	100%	Monosomy												
T642	38	32	1.6	1.8														
T657	37	34	1.7	1.8														
T661	70	33	1.5	1.7	60%	Monosomy												
T674	47	33	1.6	1.8														
T686	22	33	unchanged	unchanged			KIT	82	33	2.4	2.6	Gain						
T688	33	34	1.7	1.9														
T699	21	33	unchanged	unchanged			MET	81	34	1.6	1.7	Loss						
T717	55	33	1.6	1.8	0%	Diploid												
T744	43	33	1.6	1.8														
T750	58	33	1.6	1.7	0%	Diploid												
T771	79	33	1.5	1.7	60%	Monosomy	SMO	107	33	1.4	1.6	Loss						
T775	56	32	1.6	1.8	0%	Diploid	SMO	93	33	1.5	1.6	Loss						
T777	250	32	0.9	1														
T782	250	31	1	1.2														
T783	250	33	1	1.1			SMO	92	33	1.5	1.6	Loss						
T789	209	34	1.3	1.4														
T792	83	33	1.5	1.7	80%	Monosomy												
T795	250	33	0.9	1														
T798	173	34	1.3	1.4	0%	Diploid												
T808	204	33	1.2	1.3														
T809	17	33	unchanged	unchanged														
T823	173	32	1.3	1.4														
T850	100	33	1.5	1.6		Unanalyzable												
T941	250	33	1.1	1.2														
T1520	60	32	1.5	1.7	0%	Diploid												
T1725	9	33	unchanged	unchanged														
T826	8	33	unchanged	unchanged														
T828	223	33	1.2	1.3														
T829	250	32	1.1	1.2			KIT	87	33	2.4	2.6	Gain						
T830	21	34	unchanged	unchanged														
T834	250	33	1.1	1.2			AKT1	136	29	1.1	1.3	Loss						
T839	112	33	1.4	1.6	0%	Diploid												

Supplementary Table 3 Detail of mutation analysis

Tumor ID	Gene	Position	Amino acid change	Mutation variant	SNV/Indel	COSMIC ID	dbSNP ID	BioReT System Variant frequency	BioReT System Read depth	GeneRead Variant frequency	GeneRead Filtered Coverage
T252	NF2	30000017	p.Phe11fs/c.31_41delTTCAGCTCTCT	frameshift_variant	del	-	-	0.19096	2256	N/A	N/A
T760	NF2	30035198	p.Gln121fs/c.361delC	frameshift_variant	del	-	-	0.72631	2733	0.727	1368
T764	AKT1	105246551	p.Glu17Lys/c.49G>A	missense_variant	SNV	COSM33765	rs121434592	0.38267	7905	0.38	3839
T764	TRAF7	2225556	p.Asn520Ser/c.1559A>G	missense_variant	SNV	COSM1578119	-	0.34797	2379	0.347	1168
T138	TRAF7	2226296	p.Gln637Glu/c.1909C>G	missense_variant	SNV	-	-	0.22386	2445	0.222	1758
T275	NF2	30067938	c.1123G>C	splice_donor_variant	SNV	-	-	0.50549	3461	0.506	1717
T679	TRAF7	2225556	p.Asn520Ser/c.1559A>G	missense_variant	SNV	COSM1578119	-	0.38429	1198	0.388	598
T679	KLF4	110249348	p.Lys409Gln/c.1225A>C	missense_variant	SNV	COSM248828	-	0.38487	1803	0.384	887
T700	TRAF7	2226146	p.Lys615Glu/c.1843A/G	missense_variant	SNV	COSM1578115	-	N/A	N/A	0.315	2478
T700	KLF4	110249348	p.Lys409Gln/c.1225A>C	missense_variant	SNV	COSM248828	-	0.31604	4560	0.32	2254
T709	AKT1	105246551	p.Glu17Lys/c.49G>A	missense_variant	SNV	COSM33765	rs121434592	0.26245	4663	0.259	2304
T752	TRAF7	2226309	p.Arg641His/c.1922G>A	missense_variant	SNV	COSM673838	-	0.34039	3213	0.342	2388
T752	KLF4	110249348	p.Lys409Gln/c.1225A>C	missense_variant	SNV	COSM248828	-	0.37299	3920	N/A	N/A
T766	NF2	30061007	p.Ile280_Asp281fs/c.840_841insTGATGTCTTCAAGTTTAACTCCTCAAAGCTTC	frameshift_variant	ins	-	-	0.53405	3157	0.54	1560
T31	NF2	30054251	p.Arg225fs/c.674delG	frameshift_variant	del	-	-	0.5515	7077	0.555	3570
T65	NF2	30032818	p.Gln65*/c.193C>T	stop_gained	SNV	COSM22328	-	0.75033	12786	0.749	6403
T87	NF2	30061052	p.Leu295fs/c.885delG	frameshift_variant	del	-	-	0.46749	3983	0.468	1998
T91	NF2	30035078	c.241G>C	splice_acceptor_variant	SNV	-	-	0.38024	3392	0.378	1697
T192	NF2	30000041	p.Pro19fs/c.55_56delCC	frameshift_variant	del	-	-	N/A	N/A	0.699	4196
T237	NF2	30035201	p.Gln121Gln/c.363G>A	splice_region_variant	SNV	-	-	0.6103	5341	0.609	2631
T321	NF2	30032867	c.241T>G	splice_donor_variant	SNV	-	-	0.42643	3596	0.422	1775
T325	NF2	30038275	c.448delT	splice_donor_variant	del	-	-	0.89538	1061	0.899	1077
T369	NF2	30000033	p.Arg16fs/c.47delG	frameshift_variant	del	-	-	0.29858	4354	0.304	2154
T387	NF2	30035181	p.Gln115fs/c.344delA	frameshift_variant	del	-	-	0.61239	5183	0.618	2591
T398	NF2	30032739	c.115G>T	splice_acceptor_variant	SNV	COSM29741	-	0.5161	5814	0.515	2907
T413	NF2	30038193	p.Lys123del/c.367_369delAAG	inframe_deletion	del	-	-	0.62428	4349	0.626	2179
T415	NF2	30000085	p.Met33_Glu34fs/c.99_100insG	frameshift_variant	ins	-	-	0.26074	4794	0.259	2399
T415	NF2	30067816	p.Met334fs/c.1002delG	frameshift_variant	del	-	-	0.28858	3292	0.287	1653
T496	NF2	30069319	p.Ala395fs/c.1185delA	frameshift_variant	del	COSM24541	-	0.24273	6530	0.244	3248
T650	NF2	30038218	p.Ile131fs/c.392delT	frameshift_variant	del	-	-	0.72139	6073	0.723	3087
T690	NF2	30070820	p.Arg447fs/c.1341_1345delGCAGG	splice_acceptor_variant	del	-	-	0.39772	5270	0.399	2698
T666	TRAF7	2225556	p.Asn520Ser/c.1559A>G	missense_variant	SNV	COSM1578119	-	0.3927	2086	0.399	1063
T666	KLF4	110249348	p.Lys409Gln/c.1225A>C	missense_variant	SNV	COSM248828	-	0.37566	3034	0.391	1539
T1167	NF2	30038200	p.Gln125*/c.373C>T	stop_gained	SNV	COSM22431	-	0.39061	3948	0.382	1893
T684	NF2	30051584	p.Val173fs/c.519delA	frameshift_variant	del	-	-	0.69149	927	0.717	494
T780	NF2	30032738	c.115A>C	splice_acceptor_variant	SNV	-	-	0.66497	5324	N/A	N/A
T54	NF2	30064380	p.Ser315fs/c.945delT	frameshift_variant	del	-	-	0.47283	7072	0.496	3512
T251	NF2	30067839	p.Glu342*/c.1024G>T	stop_gained	SNV	-	-	0.63871	3500	0.635	1642
T396	SMO	128850341	p.Trp535Leu/c.1604G>T	missense_variant	SNV	COSM13146	rs121918347	0.40434	4630	0.382	1825
T407	NF2	30038168	c.364_381delTCTCCCTTGTTGCTCCTT	splice_region_variant	del	-	-	0.32615	3668	0.343	1999
T467	NF2	30064312	p.Ile296fs/c.886_904delTGGCCACAGATTCTCCAGC	splice_acceptor_variant	del	-	-	0.26552	2093	0.272	1190
T518	AKT1	105246551	p.Glu17Lys/c.49G>A	missense_variant	SNV	COSM33765	rs121434592	0.35182	6679	0.34	2993
T518	TRAF7	2226309	p.Arg641His/c.1922G>A	missense_variant	SNV	COSM673838	-	0.21678	3133	0.213	2162
T524	TRAF7	2223954	p.Gly390Arg/c.1168G>C	missense_variant	SNV	-	-	0.35208	7003	N/A	N/A
T603	NF2	30038225	p.Cys133_Pro134fs/c.399_400insC	frameshift_variant	ins	-	-	0.32229	5144	N/A	N/A
T603	NF2	30038229	p.Pro134Pro/c.402T>C	synonymous_variant	SNV	COSM4414623	-	0.33028	5144	0.326	2531
T629	NF2	30051658	p.Arg198*/c.592C>T	stop_gained	SNV	COSM22432	-	0.31326	5868	N/A	N/A
T688	TRAF7	2226313	p.His642Gln/c.1926C>G	missense_variant	SNV	-	-	0.36361	2945	0.36	2090
T688	KLF4	110249348	p.Lys409Gln/c.1225A>C	missense_variant	SNV	COSM248828	-	0.36889	4199	0.377	2193
T717	TRAF7	2225556	p.Asn520Ser/c.1559A>G	missense_variant	SNV	COSM1578119	-	0.37475	2569	0.387	1158
T717	KLF4	110249348	p.Lys409Gln/c.1225A>C	missense_variant	SNV	COSM248828	-	0.36113	6809	N/A	N/A
T744	AKT1	105246551	p.Glu17Lys/c.49G>A	missense_variant	SNV	COSM33765	rs121434592	0.39431	11508	0.374	4671
T744	TRAF7	2225603	p.Gly536Ser/c.1606G>A	missense_variant	SNV	COSM1578118	-	0.39522	5113	0.379	1968
T775	TRAF7	2225614	p.Gln539His/c.1617G>C	missense_variant	SNV	-	-	0.32011	2154	0.321	1094
T775	KLF4	110249348	p.Lys409Gln/c.1225A>C	missense_variant	SNV	COSM248828	-	0.34381	7811	0.377	3188
T782	NF2	30070883	p.Arg467fs/c.1399_1417delAGAGCCAAGCAGAAGCTCC	frameshift_variant	del	-	-	0.44797	5224	0.468	2703
T783	NF2	30069333	p.Gln400*/c.1198C>T	stop_gained	SNV	COSM22210	-	0.56734	15592	0.541	6870
T795	NF2	30032772	p.Val50fs/c.148_149delGT	frameshift_variant	del	-	-	0.48778	12852	0.492	6406
T798	NF2	30051658	p.Arg198*/c.592C>T	stop_gained	SNV	COSM22432	-	0.51731	4863	N/A	N/A
T808	NF2	30035110	p.Pro91fs/c.273_300delAGTCACCTTTCACTTCTTGGCCAAATTT	frameshift_variant	del	-	-	0.25136	4217	0.254	2127
T809	AKT1	105246551	p.Glu17Lys/c.49G>A	missense_variant	SNV	COSM33765	rs121434592	0.4318	9350	0.425	4476
T809	TRAF7	2225556	p.Asn520Ser/c.1559A>G	missense_variant	SNV	COSM1578119	-	0.39987	3168	0.403	1560
T823	NF2	30035188	p.Leu117fs/c.351delA	frameshift_variant	del	-	-	0.54959	8490	0.554	4224
T850	NF2	30032818	p.Gln65*/c.193C>T	stop_gained	SNV	COSM22328	-	0.26846	17618	0.27	9026
T1520	TRAF7	2226298	p.Gln637His/c.1911G>T	missense_variant	SNV	-	-	0.35334	1919	0.352	1375
T1725	TRAF7	2225363	p.Cys483Ser/c.1448G>C	missense_variant	SNV	-	-	0.39875	11727	0.372	5677
T826	TRAF7	2223805	p.Ile368Ser/c.1103T>G	missense_variant	SNV	-	-	N/A	N/A	0.314	1965
T826	KLF4	110249348	p.Lys409Gln/c.1225A>C	missense_variant	SNV	COSM248828	-	0.29935	5747	0.308	2870
T828	NF2	30060978	p.Phe271fs/c.811delT	frameshift_variant	del	-	-	0.63382	10122	0.64	5169
T834	NF2	30067899	p.Gln362*/c.1084C>T	stop_gained	SNV	COSM22250	rs74315498	0.67629	3958	0.682	2022
T839	NF2	30032818	p.Gln65*/c.193C>T	stop_gained	SNV	COSM22328	-	0.39869	15865	0.402	8133

Supplementary Table 4. Clinicopathological and genetic findings and their association with recurrence

Variables	Number of patients (%)	Number of recurrences (%)	RFS (%±SD)		Univariate analysis			Multivariate analysis		
			5 years	10 years	HR	95% CI	*P* value	HR	95% CI	*P* value
Age										
≤55 years	44 (49%)	13 (30%)	52%±12%	43%±12%	1.0					
>56 years	46 (51%)	17 (37%)	64%±10%	43%±12%	0.87	0.41–1.88	0.727			
Sex										
Male	29 (32%)	11 (38%)	42%±14%	28%±15%	1.0					
Female	61 (68%)	19 (31%)	67%±9%	51%±10%	0.52	0.24–1.18	0.114			
Simpson grade										
I-II	52 (63%)	9 (17%)	74%±10%	62%±14%	1.0			1.0		
III-V	30 (37%)	13 (43%)	18%±11%	-	4.48	1.77–12.81	**0.002**	3.94	1.49–11.65	**0.005**
Ki-67 labeling index										
< 4%	57 (63%)	13 (23%)	68%±10%	45%±13%	1.0			1.0		
≥ 4%	33 (37%)	17 (52%)	48%±11%	40%±12%	1.92	0.92–4.17	0.082	2.96	0.53–18.65	0.228
WHO grade										
I	69 (77%)	15 (22%)	74%±8%	50%±12%	1.0			1.0		
II-III	21 (23%)	15 (71%)	26%±11%	26%±11%	4.07	1.89–8.95	**< 0.001**	4.94	0.89–32.65	0.070
Genotype										
TRAKLS type	18 (20%)	0 (0%)	100%	100%	1.0			1.0		
NF2 type	52 (58%)	25 (48%)	50%±9%	30%±10%	2.03E+9	2.45–*	**0.003**	2.60E+9	2.05–*	**0.008**
NOC type	20 (22%)	5 (25%)	63%±19%	63%±19%	1.14E+9	1.18–*	**0.036**	7.97E+8	0.50–*	0.133

Only patients with follow-up data available were included. RFS, recurrence-free survival; SD, standard deviation; HR, hazard ratio; CI, confidence interval.
* Not be calculated.